The significance of vertical land movements at convergent plate boundaries in probabilistic sea-level projections for AR6 scenarios: The New Zealand case.

T. Naish[1], R. Levy[1,2], I. Hamling,[2], G. Garner[3,4], S. Hreinsdottir[2], R. Kopp[3], N. Golledge[1], R. Bell[5,6], R. Paulik[7], J. Lawrence[8], P. Denys[9], T. Gillies[10], S. Bengtson[2], K. Clark[2], D. King[1], N. Litchfield[2], R. Newnham[1], L. Wallace[2].

[1]Antarctic Research Centre, Victoria University of Wellington, PO Box, 600, Wellington 6140, New Zealand

[2] GNS Science, 1 Fairway Drive, Avalon, Lower Hutt, New Zealand

[3] Department of Earth and Planetary Sciences and Rutgers Institute of Earth, Ocean, and Atmospheric Sciences, Rutgers University, New Brunswick, NJ 08901, USA

[4] Gro Intelligence Ltd., 505 Park Avenue, 12th Floor, New York, NY 10022 USA

[5] Bell Adapt Ltd., Hamilton 3210, New Zealand

[6] Environmental Planning Programme, School of Social Sciences, University of Waikato, Hamilton 3216, New Zealand.

[7] National Institute of Water and Atmosphere - NIWA, 301 Evans Bay Parade, Hataitai, Wellington 6021, New Zealand

[8] Climate Change Research Institute, Victoria University of Wellington, PO Box, 600, Wellington 6140, New Zealand

[9] School of Surveying, University of Otago, PO Box 56, Dunedin 9016, New Zealand

[10]Toha – Takiwā, 11 Bright Street, Gisborne 4010, New Zealand

Corresponding author: timothy.naish@vuw.ac.nz

Key Points:

- Anticipating impacts of sea-level rise for active tectonic margins requires location-specific knowledge of vertical land movement (VLMs).
- We ingest VLMs measured continuously along a tectonically-dynamic coastline into IPCC AR6 projections to provide relative sea-level.
- Downward VLM > 2 mm y^{-1} makes a significant contribution to RSL projections bringing forward adaptation decision thresholds by decades.

Abstract

Anticipating and managing the impacts of sea-level rise for nations astride active tectonic margins requires rates of sea surface elevation change in relation to coastal land elevation to be understood. Vertical land motion (VLM) can either exacerbate or reduce sea-level changes with impacts

varying significantly along a coastline. Determining rate, pattern, and variability of VLM near coasts leads to a direct improvement of location-specific relative sea level (RSL) estimates. Here, we utilise vertical velocity field from interferometric synthetic aperture radar (InSAR) data, calibrated with campaign and continuous Global Navigation Satellite System (GNSS), to determine the VLM for the entire coastline of New Zealand. Guided by existing knowledge of the seismic cycle, the VLM data infer long-term, interseismic rates of land surface deformation. We build probabilistic RSL projections using the Framework for Assessing Changes to Sea-level (FACTS) from IPCC Assessment Report 6 and ingest local VLM data to produce RSL projections at 7435 sites, thereby enhancing spatial coverage that was previously limited to four tide gauges. We present ensembles of probability distributions of RSL for *medium confidence* climatic processes for each scenario to 2150 and *low confidence* processes to 2300. For regions where land subsidence is occurring at rates >2mm yr^{-1} VLM makes a significant contribution to RSL projections for all scenarios out 2150. Beyond 2150, for higher emissions scenarios, the land ice contribution to global sea level dominates. We discuss the planning implications of RSL projections, where timing of threshold exceedance for coastal inundation can be brought forward by decades.

Plain Language Summary

This study is the first to outline an approach for deriving projections of relative sea-level change that account for changes in land surface elevation continuously along a coastline. Previous sea-level projections that included vertical land movements (VLMs) were restricted to tide gauge locations. In order to increase spatial-resolution, required by practitioners for effective adaptation planning, we have combined elevations measured using satellite radar data with measurements from land-based Global Navigation Satellite System (GNSS) receivers to build a continuous VLM database showing land uplift and subsidence (sinking) for the entire coastline of New Zealand. We input this data into latest probabilistic projection methodology used in Intergovernmental Panel on Climate Change (IPCC) Assessment Report 6 (AR6) for the range of future climate scenarios. Our approach should be applied to any region of the world where the coastline is affected by active tectonic processes. Downward land movement > 2 mm y^{-1} makes a significant contribution in sea-level projections for all climate scenarios out to the end of this century. This means that adaptation planning decision thresholds, such as those linked to the impacts of coastal flooding and inundation, may be brought forward by decades.

1 Introduction

1.1 Background

Sea-level rise is one of the clearest planet-wide consequences of climate change. It impacts our communities and ecosystems, both through permanent inundation of the lowest-lying areas and by increasing the frequency of storm surge affecting the wider coastal environment. Future global mean sea-level (GMSL) rise will be controlled primarily by the thermal expansion of ocean water and mass wasting of land ice from glaciers, ice caps, and ice sheets, the latter is already dominating GMSL rise at an accelerating rate (Fox-Kemper et al., 2021).

New Zealand is one of many countries with extensive coastlines that sit astride a convergent tectonic plate boundary (Fig. 1), where large changes in land surface elevation can dramatically reduce or increase the rate of climate change driven sea-level rise. The magnitude and direction of vertical land motion (VLM) can change across short distances, resulting in highly variable rates of relative sea level (RSL) and different impacts across short sections of coastline (Conrad, 2013; Douglas, 2001; Milne et al., 2009; Stammer et al., 2013; Wöppelmann & Marcos, 2016). Accurately determining the rate and pattern of VLM along coastlines can improve location-specific RSL estimates (Cazenave et al., 1999; Ray et al., 2010; Santamaría-Gómez et al., 2017) and projections (Kopp et al., 2014) with significant implications for adaptation planning and risk management.

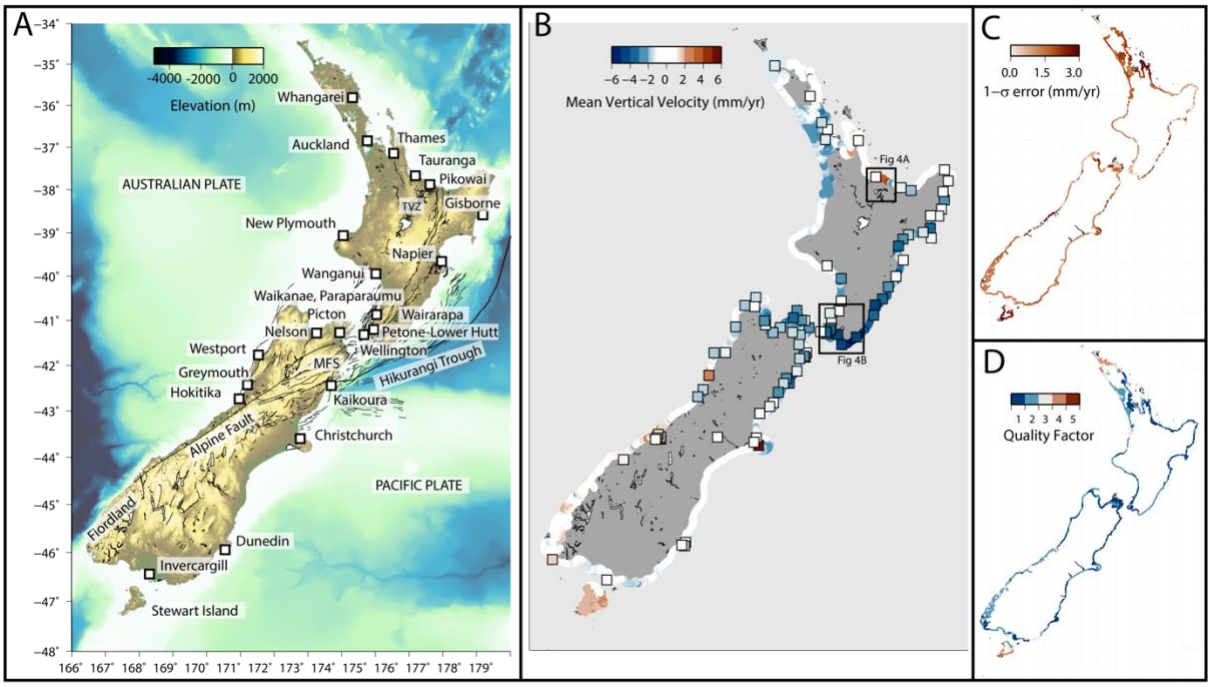

Figure 1. (A) Major tectonic features of the New Zealand convergent plate boundary setting and locations mentioned in text. MFZ = Marlborough Fault Zone. TVZ = Taupo Volcanic Zone. (B) Mean vertical velocity of the (positive upwards) land surface derived from InSAR data (Hamling et al., 2022) averaged for 2 km-spaced sites around the coastline of New Zealand. Boxes show the location of GNSS sites used to calibrate InSAR data. Note that parts of the coastline (50%) coloured white are relatively stable and LSL projections are less affected by VLM. (C) One sigma uncertainty for vertical velocity of the land surface derived from InSAR data averaged for 2 km-spaced sites. (D) Quality factor for vertical velocity of the land surface derived from InSAR data averaged for 2 km-spaced sites (1=good, 5=poor).

1.2 The role of VLM in RSL changes

The spatial variability of RSL change arises from climatic drivers and non-climatic geological processes (Gregory et al., 2019). Climatic processes include non-uniform changes in sea-surface height due to: (i) atmospheric circulation that affects air pressure (Hamlington et al., 2020; Royston et al., 2018), (ii) ocean dynamics that affect salinity and heat content (Levermann et al., 2005; Yin

et al., 2009), and (iii) perturbations in the Earth's gravitational field, rotational axis, and crustal height through viscoelastic deformation (referred to as GRD), in response to contemporary redistribution of mass between ice sheets and the ocean (Kopp et al., 2014; Kopp et al., 2010; Mitrovica et al., 2011; Riva et al., 2017; Slangen et al., 2014). Processes listed in (iii) are also referred to as the sea-level fingerprint (Mitrovica et al., 2011) or static-equilibrium effects (Kopp et al., 2014).

Non-climatic processes include: (i) isostatic adjustment following erosion (England & Molnar, 1990; Small & Anderson, 1995), (ii) sediment loading (Ivins et al., 2007), (iii) changes in mantle flow or dynamic topography (Faccenna & Becker, 2010; Hoggard et al., 2016; Kreemer et al., 2020; Moucha et al., 2008; Müller et al., 2018), and (iv) tectonic processes (Beavan & Litchfield, 2012; Hamling et al., 2022; Houlié & Stern, 2017). Shorter-term unsteady non-climatic VLM changes can also arise due to subsidence from extraction within aquifers (Erban et al., 2014; Galloway & Burbey, 2011; Herrera-García et al., 2021) and hydrocarbon reservoirs (Chaussard et al., 2013; White & Morton, 1997), the weight of cities (Han et al., 2020; Jiang et al., 2021; Parsons, 2021) and sediment compaction (Carbognin & Tosi, 2002; Dixon et al., 2006; Johnson et al., 2018). For cratonic continental margins in the Northern Hemisphere, the most significant non-climatic contribution to VLM is the viscoelastic response of the crust arising from glacial isostatic adjustment (GIA) to the loss of continental ice sheets since the Last Glacial Maximum (LGM; c. 18 ka) (Caron et al., 2018; Farrell & Clark, 1976; Milne & Mitrovica, 1998; Peltier et al., 2015).

For convergent margin coastlines in the far-field of the polar ice sheets, where the effect of GIA is small, tectonic processes are the greatest influence on VLM, and therefore RSL variability. These processes cause rapid, non-linear VLM changes during and just following earthquakes. Longer-term steady uplift or subsidence occurs through elastic deformation between seismic events (Burgette et al., 2009; Denys et al., 2020; Mazzotti & Stein, 2007) and/or aseismic creep or slow slip events (SSEs) associated with subduction zones (Wallace, 2020; Wallace & Beavan, 2010; Wallace et al., 2012). These long-term interseismic tectonic VLMs may continue with the same sign (up or down) for decades to centuries and in some cases at rates that exceed the GMSL rise projected for the coming decades (IPCC AR6). A previous assessment of VLM around the New Zealand coastline (Beavan & Litchfield, 2012) noted the probability that a high-magnitude earthquake will cause large vertical displacement at any given point along the coastline over the next 100 years, is low due to historic lengths of the earthquake cycle (Stirling et al., 2012). Therefore, the interseismic rate is dominant across decadal time scales and is most useful when estimating sea-level rise over the next century. Nevertheless, the effect of potential future vertical land-level changes due to earthquake cycle processes and coseismic displacement should be considered. This is particularly important for high probability events including an Alpine Fault rupture (Fig. 1) and large subduction event on the Hikurangi subduction zone, which respectively have a 75% and 26% likelihood of producing a large earthquake in the next 50 years (Howarth et al., 2021; Pizer et al., 2021). However, we note that the amount and direction of any VLM associated with these events is difficult to predict and that historical fault ruptures on the Alpine Fault are predominantly strike-slip and produce very little VLM in the South Island. Whereas the earthquake 'effect' on future sea level should be evaluated in a probabilistic sense, similar to the way that probabilistic seismic hazard models are implemented (Gerstenberger et al., 2020), such work is beyond the scope of this study.

Traditionally, sea-level projections in guidance documents used by coastal zone planners and practitioners did not account for local VLM (Church et al., 2013; Gornitz et al., 2019; Horton et al., 2011; Katsman et al., 2011; Lawrence et al., 2018; Ministry for the Environment, 2017; National Research Council, 2012; Perrette et al., 2013; Slangen et al., 2014; Slangen et al., 2012). More recently, probabilistic sea-level projections that characterize plausible Bayesian probability distributions of future climate scenarios (Meinshausen et al., 2020) to estimate GMSL and RSL (Fox-Kemper et al., 2021; Jackson & Jevrejeva, 2016; Kopp et al., 2014; Kopp et al., 2016) include VLMs extracted from historical tide-gauge data (Kopp et al., 2014). However, users are more frequently demanding high-resolution, spatially resolved RSL projections, particularly along coastlines where VLMs are significant and highly variable (e.g., New Zealand where rates vary from –8 to +10 mm y^{-1}) (Hamling et al., 2016; Hamling et al., 2022; Houlié & Stern, 2017; Lamb & Smith, 2013). By utilizing space-borne geodetic techniques, to include installing permanent Global Navigation Satellite System (GNSS) antenna at or near tide gauges, we have revolutionised our ability to separate terrestrial drivers of relative sea level change from climate and ocean signals (Blewitt et al., 2010; Denys et al., 2020; Poitevin et al., 2019). However, most permanent GNSS stations are not co-located with the tide gauges (Hamlington et al., 2016; Santamaría-Gómez et al., 2017) and GNSS information is spatially limited. In order to increase spatial-resolution, InSAR velocity data calibrated by high-precision campaign and continuous GNSS measurements are being used to build velocity fields of land deformation along the coastal strip (Biggs & Wright, 2020). This approach is providing unprecedented granularity with significantly reduced uncertainties (Hamling et al., 2022; Poitevin et al., 2019).

1.3 Aims of this study

This study was designed in response to a need for relative sea level projections at high spatial resolution that accommodate highly variable rates of vertical land movement along New Zealand's coastal margin. We utilise a high-resolution vertical velocity field generated for the period 2003-2011 from Envisat InSAR data that are calibrated with campaign and continuous GNSS time series through the same interval (Hamling et al., 2022). These data are used to establish VLM estimates for 7435 sites spaced ~2 km apart around the New Zealand coastline. We generate probabilistic RSL projections for each site using the Framework for Assessing Changes to Sea-level (FACTS) (Fig. 2) (See Methods in Supporting Information). FACTS is based on the projection methodology (Garner et al., 2021; Kopp et al., 2014; Kopp et al., 2016) and was used for the Intergovernmental Panel on Climate Change WGI 6th Assessment Report (Fox-Kemper et al., 2021). Here we replace the non-climatic background module of Kopp et al. (2013; 2014) with VLM data from Hamling et al., (2022). We use the IPCC AR6 approach and present an ensemble of probability distributions of RSL for *medium confidence* processes for Shared Socioeconomic Pathways (SSP) scenarios to 2150 and *low confidence* processes in SSPs to 2300 (see Methods in Supporting Information). These new local "NZSeaRise" projections can be accessed through a web-based GIS-visualisation tool (www.searise.nz/maps-2).

New Zealand's coastal hazard and climate change guidance for local government (Lawrence et al., 2018; Ministry for the Environment, 2017) currently uses four sea-level rise scenarios that are drawn from the probabilistic projections of Kopp et al. (2014) and apply a regional sea-level departure from GMSL. These projections indicate that sea level could rise by as much as 1.2 m by 2110 under a high emissions scenario (the 83rd percentile of RCP8.5). However, the guidance

does not provide specific allowances for local, non-climatic/oceanic factors due to tectonics, land compaction, or sediment accumulation, and it cautions that "users will also need to factor in a local component for VLM…" (p. 102). As discussed in Section 1.2, VLMs contribute considerably to the magnitude of RSL rise this century, with subsidence rates in some localities as much as 8 mm y^{-1} (Hamling et al., 2022). While the primary purpose of this paper is to outline a methodology for the inclusion of high-resolution, high-precision, satellite-borne geodetic VLM data into probabilistic sea-level projections and their use, we also provide a scientific basis for a new set of location-specific sea-level projections utilising IPCC AR6 WGI for use by practitioners (insert link to MfE interim guidance website here) that will underpin adaptation planning decisions in New Zealand.

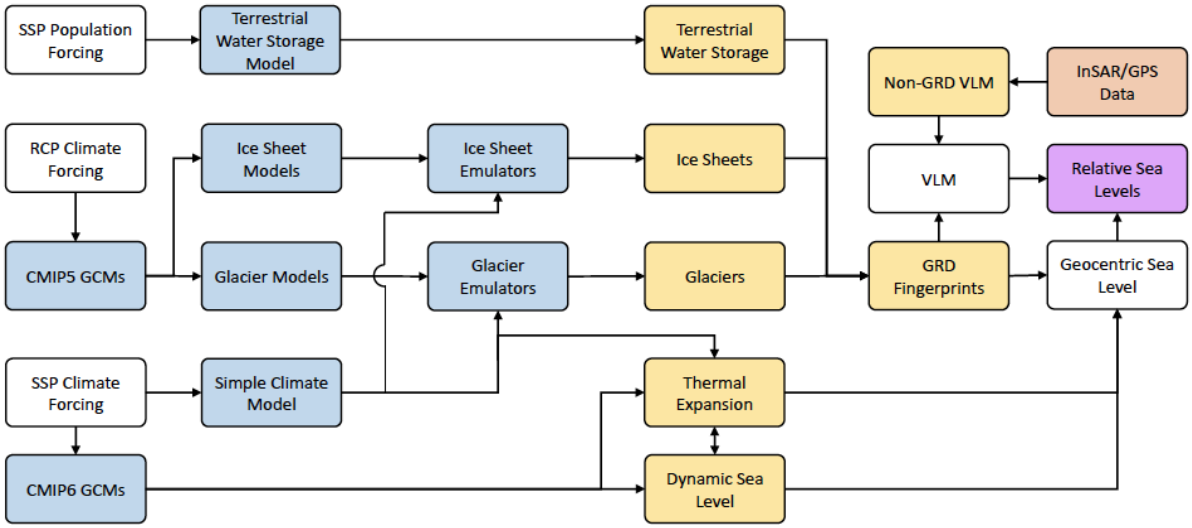

Figure 2. Logical flow of sources of information within the Framework for Assessing Changes to Sea-level (FACTS) to estimate RSL projections (explained in Methods in Supporting Information).

2. Regional Geological and Geographical Context

2.1 Plate tectonic setting and influence on VLM

Oblique convergence between the Pacific and Australian plates at rates of 30 - 40 mm y^{-1} has produced a complex plate boundary with a variety of tectonic regimes operating on a range of temporal and spatial scales that affect the length of New Zealand in different ways (Fig. 1A). In the North Island, tectonics and contemporary deformation are dominated by westward subduction of the Pacific plate along the Hikurangi trough (Nicol et al., 2007; Wallace et al., 2004). Along the Hikurangi margin, block modelling of campaign GNSS data suggests a that the northern Hikurangi margin is dominated by aseismic creep and slow slip, while deep interseismic coupling occurs on the southern Hikurangi margin, to depths of 30 - 40 km (Wallace & Beavan, 2010; Wallace et al., 2004). Plate interface coupling drives long-term regional subsidence of the east and south coasts of the lower North Island at rates up to 8 mm y^{-1}. Episodic, aseismic Slow Slip Events (SSEs) on the subduction zone produces short term reversals (mm to multi-cm) in VLM ranging from weeks to years (Wallace & Beavan, 2010; Wallace et al., 2012). Uplift due to SSEs is difficult to constrain due to limited continuous GNSS (cGNSS) across the Wellington region (Fig. 1A, 1B; see section

2.2), but is estimated to have offset approximately one third of the secular subsidence between 1996-2016 in regions where they occur (Denys et al., 2020). Average long-term (net) VLMs between -2 to -5 mm y^{-1} are estimated for this region (Hamling et al., 2022) (Fig. 3A).

In the northern South Island, 80% of plate motion is taken up along four major strike slip faults through the Marlborough Fault Zone (MFZ, Fig.1A) (Holt & Haines, 1995; Langridge & Berryman, 2005; Van Dissen & Yeats, 1991; Wallace et al., 2007). Further south, 70-75% of the Pacific-Australia relative motion is taken up along the Alpine Fault with the remainder accommodated across the South Island (Wallace et al., 2007). The convergent component of motion has led to the growth of the Southern Alps at rates of between 5-9 mm y^{-1} (Beavan et al., 2010; Beavan et al., 1999; Little et al., 2005; Michailos et al., 2020; Norris & Cooper, 2001; Sutherland et al., 2006).

Along at least half of New Zealand's ~15,000 km coastline from Christchurch clockwise to Hokitika and from Whanganui clockwise to Tauranga (except for Auckland/Waikato segment) estimates of VLM rate from geological archives (spanning the last 125,000 years) are relatively low (<2 mm y^{-1}) and are consistent within error of the GNSS rates (Beavan & Litchfield, 2012; Hamling et al., 2022; Houlié & Stern, 2017; Lamb & Smith, 2013; Pillans, 1986; Ryan et al., 2021). In contrast, along ~40% of the coastline including eastern and southern lower North Island and upper South Island, geodetic data show land surface subsidence has been high this century with rates between 3 to 8 mm y^{-1} (Fig. 3A). However, on longer (millennial) geological timescales these regions have generally been uplifted due to convergence and shortening across the plate boundary and the long-term aggregate effect of large earthquakes (Berryman et al., 2011; Clark et al., 2019; Howell & Clark, 2022). The remaining sections of New Zealand's coastline display complex short-wavelength variations in VLM. For example, high rates of uplift (episodically reaching 10 mm y^{-1}) occur along 30 km zone of coastline in Bay of Plenty, near Matata at the eastern margin of the TVZ rift (Fig. 3B). This rapid uplift is suggested to be associated with a transient earthquake swarm attributed to an off-axis magma body (Hamling et al., 2016; Hamling et al., 2022).

The most significant and damaging earthquake events that have affected New Zealand VLM this century include: (i) September 2010, Mw 7.1 Darfield earthquake, (ii) 22 February 2011, Mw 6.3 Christchurch earthquake, (iii) 13 June 2011, Mw 5.9 Godley Head earthquake, (iv) a sequence of earthquakes in Christchurch on 23 December 2011 (Kaiser et al., 2012), and (v) the 14th November 2016, Mw 7.8 Kaikoura earthquake (Hamling et al., 2017). The latter caused a rapid ~10 mm of subsidence at the Wellington tide-gauge cGNSS followed by a phase of uplift, which appears to have peaked during a series of SSEs on the Hikurangi margin triggered by the earthquake (Wallace et al., 2018). All these events caused rapid shifts in VLM at the Lyttleton tide gauge (Fig.1A). Two strike-slip earthquakes (Cook Strait, Seddon) on the 21st July and 16th of August 2013 respectively, had no apparent effect on the vertical component (Hamling et al., 2014) in tide guage records. Whereas, the next earthquake rupture in Christchurch (Canterbury) could be a long way off as paleoseismological data suggest the penultimate rupture on the Greendale fault (Darfield) occurred between 20 - 30 kyr ago (Hornblow et al., 2014) and that the Christchurch events are a once in 10-kyr occurrence (Mackey & Quigley, 2014).

Southwest New Zealand is also an active seismic region where the Australian plate subducts beneath the Pacific plate along the Puysegur Trench. Whereas the Dunedin tide gauge is 200 – 300 km from the region, it has been affected by recent significant large earthquakes in Fiordland including the George Sound 2007 (Petersen et al., 2009) and Dusky Sound 2009 (Beavan et al., 2010) earthquakes. In addition, the Mw 8.1 Macquarie Island 2004 event (Watson et al., 2010) affected the whole of New Zealand, but largely via horizontal deformation.

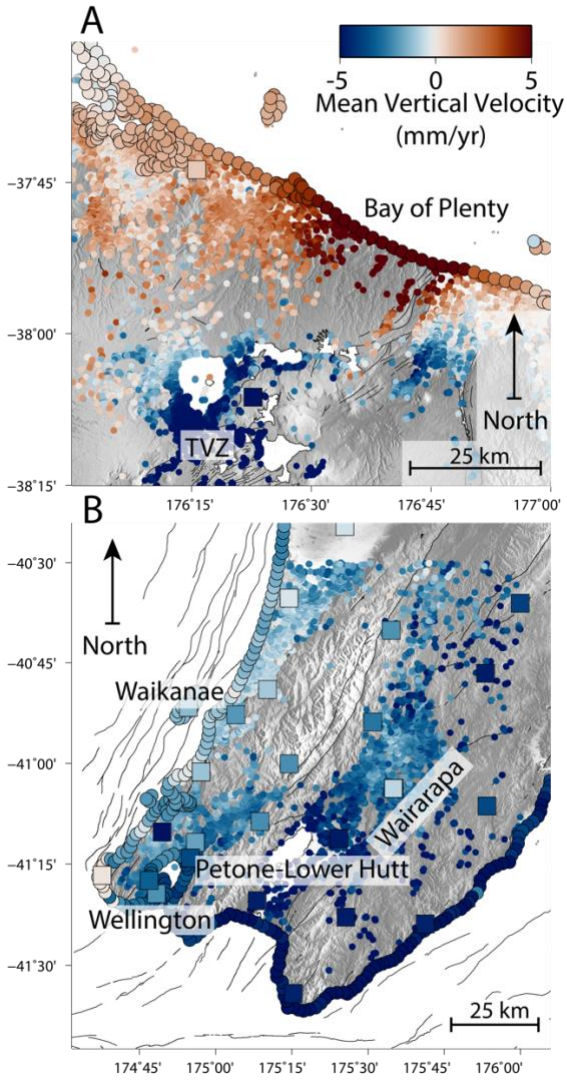

Figure 3. Mean vertical velocity (positive upwards) of the land surface derived from InSAR data averaged for 2 km-spaced sites around the coastline of (A) the Lower North Island showing high rates of subsidence and (B) eastern North Island, central Bay of Plenty showing high rates of uplift (see Fig. 1B). Boxes show the location of GNSS sites used to calibrate InSAR data.

To reduce potential temporal biases introduced by local earthquakes, the period of 2003 and 2011 was selected in this study as it largely preceded many of the Mw>6 earthquakes which have struck New Zealand since late 2009, and is therefore representative of the VLM between the seismic events. The large earthquakes in the Christchurch region in 2010 and 2011 were removed from the

InSAR time series. The inter-seismic rate is considered appropriate for the extrapolation of VLM used in the RSL projections, because over the next 100 years the probability of a high-magnitude earthquake with large local vertical displacement is low due to the historic lengths of the earthquake cycle (Beavan & Litchfield, 2012). Notwithstanding this, seismic hazard risk (Stirling et al., 2012) and the potential for rapid subsidence and/or uplift, while difficult to predict, should always be considered. For example, a major event on the ~600 km long Alpine Fault is likely (75% probability) to occur in the next 50 years (Howarth et al., 2021), but historical fault rupture data suggest little VLM will occur in the South Island. The majority of the southern east coast margin of the North Island is currently experiencing subsidence, largely due to coupling along the plate interface. Model simulations of a rupture of the entire Hikurangi margin shows the intersesimically-coupled zone beneath Wellington would experience up to 2m of subsidence, while the southern Wairarapa coast would experience uplift (Wallace et al., 2014). The spatial distribution of coseismic uplift and subsidence is highly variable and dependent on which fault or faults rupture. While parts of the margin may get a reprieve from the accumulated interseismic subsidence, other areas may have to contend with additional supporting subsidence as a result of any earthquake. In addition, large post-seismic transient deformation may follow a major event temporarily amplifying the local VLM before returning to interseismic rates in as little as 10 years (Hamling et al., 2017; Hussain et al., 2018). Consequently, in some parts of the Christchurch region post-earthquake subsidence rates are significantly higher than the pre-earthquake VLM time series. In view of these various uncertainties surrounding co-seismic VLM events, in particular their long cycles and stochastic unpredictability, secular trends for VLMs used in this paper represent long-term interseismic uplift and subsidence and are appropriate to use for shorter term (decadal) RSL projections.

2.2 Sea-level rise since 1900

Global mean sea level has risen approximately 0.18 m since 1900 and there is robust evidence that GMSL rise has accelerated over the past several decades (Dangendorf et al., 2019; Dangendorf et al., 2017; Frederikse et al., 2020). The rate of GMSL rise has doubled since 1993 (start of the satellite era) to a current global-mean estimate of 3.69 ± 0.48 mm y^{-1} (Nerem et al., 2018). The most likely cause for this acceleration is an increase in the rate of mass loss from Earth's mountain glaciers and large ice sheets (Bamber et al., 2018; Fox-Kemper et al., 2021; Shepherd et al., 2018; Velicogna et al., 2014).

Sea-level rise data for New Zealand are derived from long-term tide gauges (TG) that are co-located with continuous GNSS at four main ports (Auckland, Wellington, Lyttleton, and Dunedin). These sites provide baseline records (~ 120 years, Figs. 1A) that show an average increase in RSL of 0.21 ± 0.60 m (1.8 ± 0.5 mm y^{-1}) from 1900-2018, with a doubling since 1960 (Bell & Hannah, 2019; Hannah & Bell, 2012). The cause of this doubling remains equivocal due to complications from atmospheric and ocean dynamic influences (e.g., Interdecadal Pacific Oscillation) (Hannah & Bell, 2012). Adjustments for long-term VLM at each TG (see section 4.2) give a best estimate of absolute regional sea-level rise rate for New Zealand of $+1.45 \pm 0.28$ mm y^{-1} for the period from 1891 to 2013, with a trend increase at the Auckland TG of 0.23 ± 0.15 mm y^{-1} since 1990 (Denys et al., 2020).

Whereas the observed century scale increase of ~0.18 m in sea level may seem small and potentially inconsequential, this historical rise in GMSL has increased the frequency of coastal flooding events around the world (Lin et al., 2016). Importantly, relatively modest (0.30-0.45 m) increases in sea level over the coming decades will dramatically increase the frequency of inundation for many sections of the New Zealand coastline. For example, coastal inundation that today occurs at the 1% annual exceedance probability, will become annual events in several of New Zealand's largest cities (Paulik et al., 2020).

2.2 Primary sources of uncertainty in global mean sea-level projections

Up to 2050, GMSL projections for the range of SSPs exhibit little scenario dependence. Beyond 2050, the scenarios increasingly diverge. The AR6 projections show that processes known with at least *medium confidence*, GMSL will rise between 0.33 m and 1.02 m (17th - 83rd percentiles) above a baseline period (1995 to 2014) by 2100 for all scenarios between SSP1-2.6 and SSP5-8.5 (Fig. 4). However, the assessment also notes "that there is a substantial likelihood that sea level rise will be outside the likely range for *medium confidence* processes, and that Supporting processes, for which there is presently *low confidence*, may also contribute to (the likely range) of sea level change". Consequently, the AR6 projections also include *low confidence* projections intended to reflect contributions from these additional processes under high-emissions scenarios. In these projections GMSL for SSP5-8.5 will rise between 0.6 - 1.6 m (17th - 83rd percentile range) with the 5th - 95th percentile range extending to 0.5 - 2.3 m, leading the IPCC's Summary for Policymakers to state, that "2 m GMSL rise by 2100 cannot be ruled out".

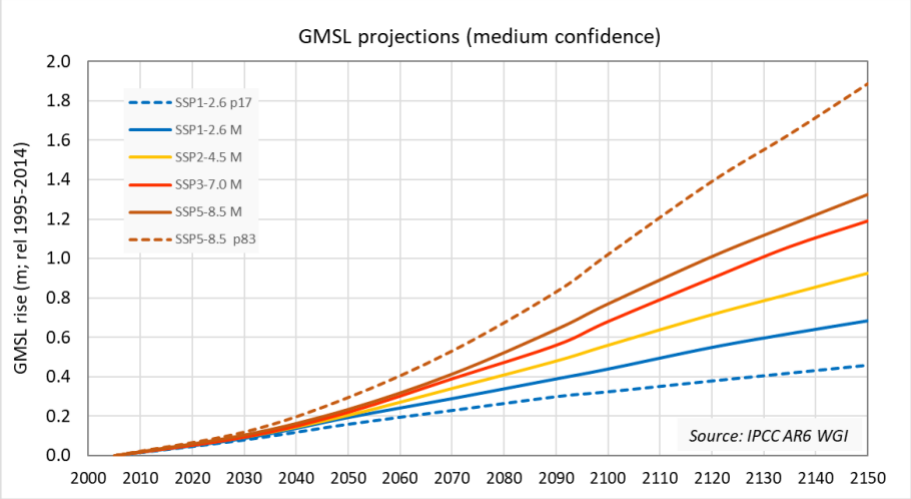

Figure 4. Median and *likely* (17th-83rd percentile) range for GMSL estimated for processes known with *medium confidence* to 2150: SSP1-2.6 (blue), SSP2-4.5 (yellow), SSP3-7.0 (red); SSP5-8.5 (magenta). Baseline reference period follows AR6 and is the mean of 1995 - 2014.

The increasing spread in the likely range of GMSL projections beyond 2050 is due in part to (a) uncertainty related to future emissions scenarios and (b) deep uncertainty due to a lack of scientific understanding of the key rate-determining processes that should be represented in dynamic ice sheet (ISM) and earth system (ESM) models and their couplings. For example, AR6 *medium*

374 *confidence* projections utilise outputs from a standardised ensemble of ISMs from the Ice Sheet
375 Model Intercomparison Project Experiment 6 (ISMIP6) (Edwards et al., 2021; Goelzer et al., 2020;
376 Nowicki et al., 2016; Seroussi et al., 2020) and the Linear Response Model Intercomparison
377 Project (LARMIP2) (Levermann et al., 2020). In contrast, the IPCC AR6 characterization of *low*
378 *confidence* processes use a smaller set of studies that adopt more heterodox approaches and
379 incorporate a single ISM output that represents Marine Ice Cliff Instability (MICI) (DeConto et
380 al., 2021) (referred to in this paper as DP21) as well as estimates from a structured expert
381 judgement (SEJ) (J. L. Bamber & Aspinall, 2013; Jonathan L. Bamber et al., 2019).
382
383 GMSL beyond 2100 continues to rise under all SSPs. Projections to 2300 based on conservative
384 extensions of *medium confidence* ISM output leads to a GMSL rise of 0.8m to 2.0 m under SSP1-
385 2.6, and 1.9 to 4.1 m under SSP5-8.5 (IPCC AR6). Using Antarctic results from a model with
386 MICI (DP21; *low confidence*) and using global warming levels equivalent to SSP1-2.6 and SSP5-
387 8.5, leads to GMSL ranges of 1.40 m to 2.10 m and 9.50 m to 15.90 m, respectively. A further
388 unstable process, known as Marine Ice Sheet Instability (MISI) is considered to cause self-
389 sustaining collapse of marine-based sectors of Antarctica's ice sheet once they begin retreating into
390 deep bedrock basins below sea-level. Models incorporating MISI imply the threshold for
391 irreversible loss is crossed at global warming above 1.5-2°C, resulting in long-term commitment
392 to millennial-duration GMSL rise (Clark et al., 2016; DeConto et al., 2021; Golledge et al., 2015;
393 Van Breedam et al., 2020). This tipping point may be avoided if global warming is stabilised in
394 line with the Paris Climate Agreement (SSP1-2.6) (DeConto et al., 2021; Golledge et al., 2015).

395 **4 Results: RSL Projections for New Zealand** (2854 words)

396

397 4.1 Large-scale patterns of sea-level change around New Zealand to 2150

398

399 Our results provide the first continuous estimates of the RSL around the entire New Zealand
400 coastline (Fig. 1) for processes known with at least *medium confidence* following AR6 for emission
401 pathways SSP1-2.6, SSP2-4.5, SSP3-7.0 SSP5-8.5 to 2150 (Fig. 4). The estimated rates and
402 magnitudes show some interesting variations due to VLM in different parts of the country (section
403 2.1). In Table S1 (Supporting Information) we provide examples of sites (Fig. 1A) that are
404 representative of the 5 highest subsidence and 5 highest uplift regions around the New Zealand
405 coastline to demonstrate the influence of VLM on LSL projections. The highest rate and magnitude
406 of RSL rise is along the eastern North Island, southern Wairarapa coast at Tora - Oroi Stream (Fig.
407 1B). Here, the likely range (17th to 83rd percentile) of RSL for all scenarios by 2150 is 1.54 m to
408 3.24 m. The near-future likely range of RSL rise by 2050 is 0.49 m to 0.72 m. In this region
409 interseismic tectonic subsidence associated with subduction coupling (section 2.1) effectively
410 doubles the decadal rate and magnitude of RSL compared with GMSL change. As noted in sections
411 2.1 & Methods (in Supporting Information), slow slip events and earthquakes on the Hikurangi
412 margin may reverse up to one third of the tectonic subsidence experienced by lower North Island
413 over the next century, and this is not accounted for in the RSL projections. Other regions where
414 tectonic subsidence significantly increases RSL rise were discussed in section 2.1 and examples
415 include northwest Nelson (eastern Tasman Bay), Kaikoura Peninsula (east coast South Island),
416 eastern Marlborough (northeast South Island) and the city of Napier (eastern. North Island)
417 (Fig.1B).
418

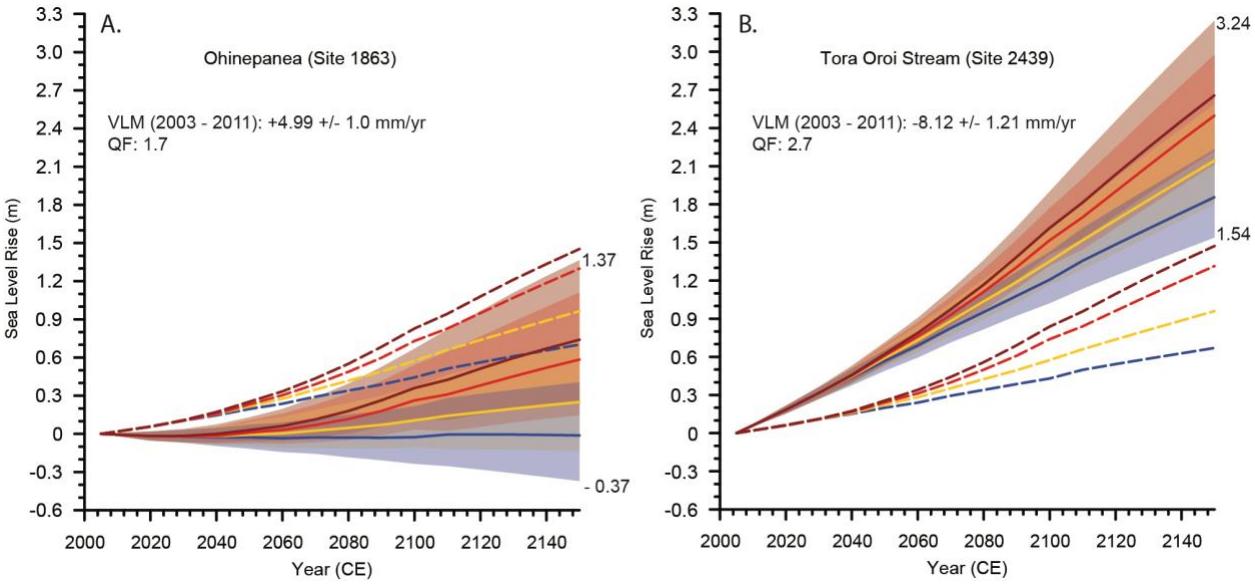

Figure 5. Projected RSL change from 2005 to 2150 at (A) Pikowai - Ohinepanea (Site 1863), the highest rate of land uplift and (B) Wairarapa Tora - Oroi Stream (Site 2439) the highest rate of land subsidence on the New Zealand coastline showing the influence of VLM for the likely range (17th-83rd percentile) for SSP1-2.6 (blue), SSP2-4.5 (yellow), SSP3-7.0 (red) SSP5-8.5 (magenta). See Fig. 1A for site locations. QF = Quality Factor (see section 3.4). Baseline reference period follows AR6 and is the mean of 1995-2014). QF = quality factor (see Supporting Information).

In contrast the lowest rate of RSL rise is along the eastern North Island, Bay of Plenty coastline near the small settlement of Ohinepanea (Fig. 5). Here, the likely range (17th to 83rd percentile) of RSL for all scenarios by 2150 is -0.37 m to 1.37 m. The near-future likely range of RSL rise by 2050 is -0.12 m to 0.13 m. In this region localised tectonic uplift associated with magmatic activity (section 2.1) largely offsets the rate and magnitude of GMSL rise over the next 50 years, and halves it over the next 100 years. Other regions where tectonic uplift significantly decreases RSL rise include lower west coast of the South Island (Fiordland), western Coromandel (North Island), and East Cape of the North Island (Fig.1A). While over longer timeframes (e.g., out to 2300) and for higher emissions scenarios, VLMs have comparatively less influence on RSL rise compared to the growing land ice contribution, they are still a significant contributor to the amplitude and rate of RSL change to 2150.

4.2 Comparing long-term tide gauge records with space-borne geodetic observations and RSL projections.

Historical tide gauge (TG) records are routinely used to determine RSL over the past century and offer a mechanism to compare with our projections where time series overlap. Here we plot TG records at Auckland (Queens Wharf), Tauranga (Moturiki), Wellington (Queens Wharf), Christchurch (Lyttleton) and Dunedin with RSL projections to 2150 (Fig. 6A). Recent analysis of the TG records used cGNSS data and inferences regarding seismic activity to estimate average VLM rates for each of the TG over the past century (Denys et al., 2020). This analysis suggests that most of the TGs have subsided at lower rates over the past century than indicated by our VLM analysis for the period between 2003 and 2011. These differences contribute to the fact that historical sea-level trends determined from TG data are less than indicated by our probabilistic projections, a feature that is most obvious at Wellington. However, observed TG trends and our sea level projections are similar over more recent periods (e.g., 1980 to 2020) (Fig. 6B). This

observation suggests either our projections overestimate the long term VLM contribution to relative sea level (at century time scales), that subsidence rates have increased over the past several decades, that the TG records have been incorrectly adjusted for local subsidence, that there may be processing and trend analysis errors, incorrect assumptions in local and global reference frame calibration, or some combination of all these factors. Future studies will provide new centennial-scale salt marsh records (Garrett et al., 2022), and together with the incorporation of recent and future observations, will lengthen time-series, reduce uncertainties, and ultimately help reconcile past, present a future VLM datasets.

Here we explore the differences between long-term and short-term TG VLM estimates in more detail. TG data from Queens Wharf in Auckland indicate an average rise in RSL of 1.57 ± 0.15 mm y^{-1} between 1900 and 2015 with a trend increase of 0.23 ± 0.15 mm y^{-1} since 1990 (Denys et al., 2020). Denys et al., (2020) calculated an average vertical velocity at the Auckland TG of -0.16 mm y^{-1} over the past century, significantly lower than the absolute vertical velocity of -0.62 ± 0.1 mm y^{-1} they measured at the co-located cGNSS unit for the interval from 2000 to 2015. The difference in short-term vs long-term rate is due to adjustments made for Glacial Isostatic Adjustment and Solid Earth Deformation (see section 3). The absolute vertical velocity determined for cGNSS stations (v_{GNSS}) by Denys et al., (2020) are relative to the ITFR08 reference frame (Collilieux & Wöppelmann, 2011; Wöppelmann et al., 2007). Here we use the updated reference frame ITRF14 (Altamimi et al., 2016) and estimate an absolute vertical velocity of -1.09 ± 0.12 mm y^{-1} at the Auckland TG for the period from 2003 to 2011 and -1.21 ± 0.03 mm y^{-1} for the period from 2001 to 2022 (Fig. 8). Hamling et al., 2022 used ITRF14 calibrated cGNSS velocities and InSAR data to estimate a VLM rate of -1.28 ± 0.07 mm y^{-1} for the region within a ~0.7 km sampling radius around the Auckland TG, which is consistent with our TG v_{GNSS} data. Whereas these velocity data indicate that reference frame choice can make a difference, they all show that the Auckland TG has been subsiding at significantly higher rates for the past 21 years than inferred for the previous century.

Our estimates of VLM at locations away from the TG and around Waitemata harbour are highly variable and have a significant influence on relative sea level projections. For example, Viaduct Basin (Port of Auckland, Site 1231; Supporting Information Table S2) is a highly developed commercial and residential area located ~ 1 km from the TG with a VLM estimate of -2.9 ± 1.1 mm y^{-1}. RSL projections for this location indicate that sea level will rise between 0.81 and 2.50 m by 2150 for the likely range of all scenarios. In contrast, our VLM estimate for the residential area at the eastern end of St Heliers Bay (Site 1249) located ~10 km from the TG, is -0.37 ± 1.5 mm y^{-1}. Assuming the VLM rate remains constant, RSL rise at this location will be ~30 to 40 cm less than at Viaduct Basin, increasing between 0.40 and 2.16 m by 2150 for the likely range of all scenarios. In general our VLM estimates suggest the Auckland region has been subsiding between ~1 and 3 mm y^{-1} over the past two decades, a range that is supported by other InSAR studies (Wu et al., 2022). The cause for this apparent relatively recent increase in subsidence and its spatial variability requires further investigation but contributing processes may include ground water extraction (Wu et al., 2022) and the increasing influence of urbanisation (Parsons, 2021).

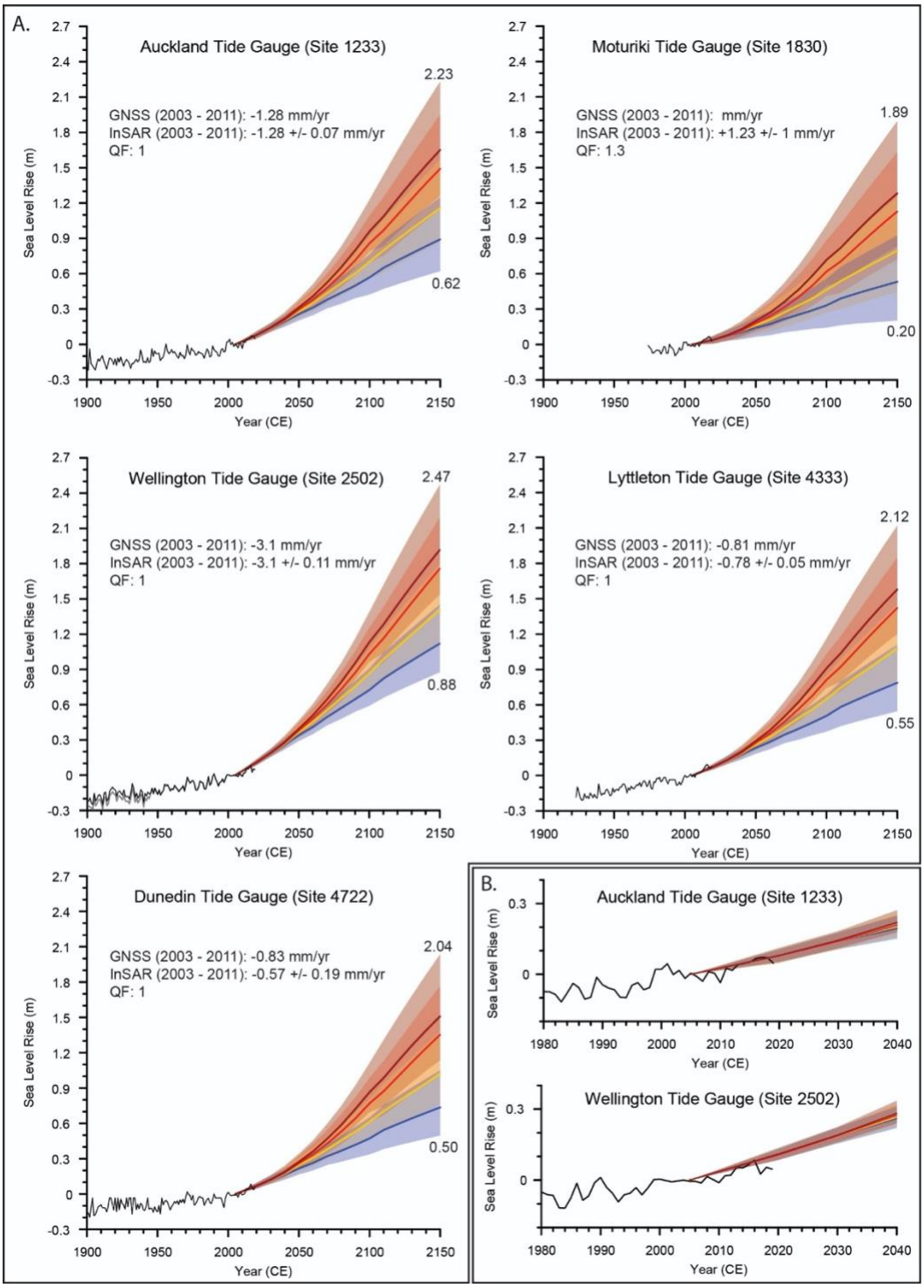

Figure 6. A. Historical records from 1900 to 2020 and RSL projections from 2005 to 2150 for processes known with medium confidence for SSP1-2.6 (blue), SSP2-4.5 (yellow), SSP3-7.0 (red), SSP5-8.5 (magenta) showing median and likely range (17th-83rd percentile) for tide gauges at Auckland, Tauranga (Moturiki), Wellington, Christchurch (Lyttleton), and Dunedin. Baseline reference period follows AR6 and is the mean of 1995-2014). QF = quality factor (see Supporting Information). B. Historical records from 1980 to 2020 and RSL projections from 2005 to 2040 for processes known with medium confidence for SSP1-2.6, SSP2-4.5, SSP3-7.0 SSP5-8.5 showing median and likely range (17th-83rd percentile) for tide gauges at Auckland and Wellington.

The inferred linear rate of RSL at the Tauranga (Moturiki) TG is 1.9 ± 0.2 mm y^{-1} (Hannah & Bell, 2012). The nearest cGNSS station is located ~ 13 km east and inland of the TG and records a vertical velocity of +0.01 ± 0.21 mm y^{-1} for the interseismic period 2003 to 2011 and -0.06 ± 0.07 mm y^{-1} for the interval from 2003 to 2022 (Fig. 7). Here we estimate an interseismic VLM rate of +1.22 ± 1 mm y^{-1} for the region within a ~0.6 km sampling radius around Site 1830 proximal to the TG. While this VLM estimate is slightly higher than the v_{GNSS} data for the same period, the estimates are consistent within error and show the region is slowly rising. Therefore, our sea level projections indicate that the region will experience a RSL rise between 0.20 and 1.90 m by 2150 for the likely range of all scenarios, values that are lower than the global mean (Fig. 6).

Reconciling long-term TG data with short-term VLM estimates in Wellington is more challenging than for other regions of New Zealand due to the local influence of tectonic events including large plate boundary ruptures and slow slip earthquakes (SSE) along the Hikurangi subduction zone (K. Clark et al., 2019; Pizer et al., 2021; Wallace & Beavan, 2010). TG data from Queens Wharf in Wellington indicate an average rise in RSL of 2.18 ± 0.17 mm y^{-1} between 1900 and 2015 (Denys et al., 2020). Denys et al., 2020 calculated an average vertical velocity at the Wellington (Queens Wharf) TG of -0.62 mm y^{-1} over the past century, significantly lower than the absolute vertical velocity of -2.84 ± 0.18 mm y^{-1} they measured for the interval from 2000 to 2015 at the cGNSS located on the national museum ~500m from the TG. The difference in their observed short-term vs calculated long-term average VLM rate is due to adjustments made for Glacial Isostatic Adjustment (v_{GIA}), Solid Earth Deformation (v_{SED}), and estimates of local uplift due to historical regional earthquake events and SSE's (v_{LOCAL} + v_{EQ}). Absolute vertical velocities at the Wellington tide gauge cGNSS calculated using ITRF14 are -2.41 ± 0.25 mm y^{-1} for the period from 2003 to 2011 and -2.94 ± 0.27 mm y^{-1} for the period from 2000 to November 2016, which includes the Christchurch earthquakes (Fig. 7) but excludes the effect of the Mw 6.3 Kaikoura earthquake (Hamling et al., 2017). Significant uplift during the Kaikoura event decreases the multi-decadal vertical velocity rate at the Wellington TG cGNSS to -1.66 ± 0.64 mm y^{-1} (Fig. 7). Data collected at the Wellington TG cGNSS following the Kaikoura event and associated afterslip and triggered SSE's (Wallace et al., 2018) show that absolute vertical velocity from 2018 to 2022 is +0.00 ± 0.2 mm y^{-1}.

Hamling et al. (2022) used ITRF14 calibrated cGNSS velocities and InSAR data to estimate an interseismic VLM rate of -3.09 ± 0.11 mm y^{-1} within a ~0.7 km sampling radius around the Wellington TG, which is slightly higher than the TG v_{GNSS} data for the same period. This rate is also approximately double the Kaikoura earthquake-adjusted rate for the period from and while subsidence is still significant over this longer time interval, our RSL projections across the Wellington region represent maximum estimates. VLM measurements at the Christchurch (Lyttleton) TG cGNSS further emphasise the effect of the earthquakes. Average cGNSS velocity at the Lyttelton TG from 2003 to 2011 is -0.92 ± 0.20 mm y^{-1} and +5.7 ± 1.8 mm y^{-1} for the period from 1999 to 2022 due to significant uplift (~10 cm) during the 22 February 2011, Mw 6.3 Christchurch earthquake (Fig. 7). In contrast to uplift at the Wellington TG, the Mw 7.8 Kaikoura earthquake caused co-seismic subsidence (~2 cm) at Lyttleton (Fig. 7). These data illustrate the challenge associated with estimating VLM for RSL projections along highly dynamic coastlines like those that characterise New Zealand (see also King et al., 2020). The potential for time-variability of vertical deformation rates in New Zealand due to coseismic (and post-seismic) deformation will be considered in a future study. Regardless, we propose that cGNSS and InSAR

data offer a more accurate and robust assessment of regional VLM for local RSL projections over the near-term (to 2100), than do longer term VLMs extracted from TG records, and should be used for coastal planning and decisions over decadal time scales.

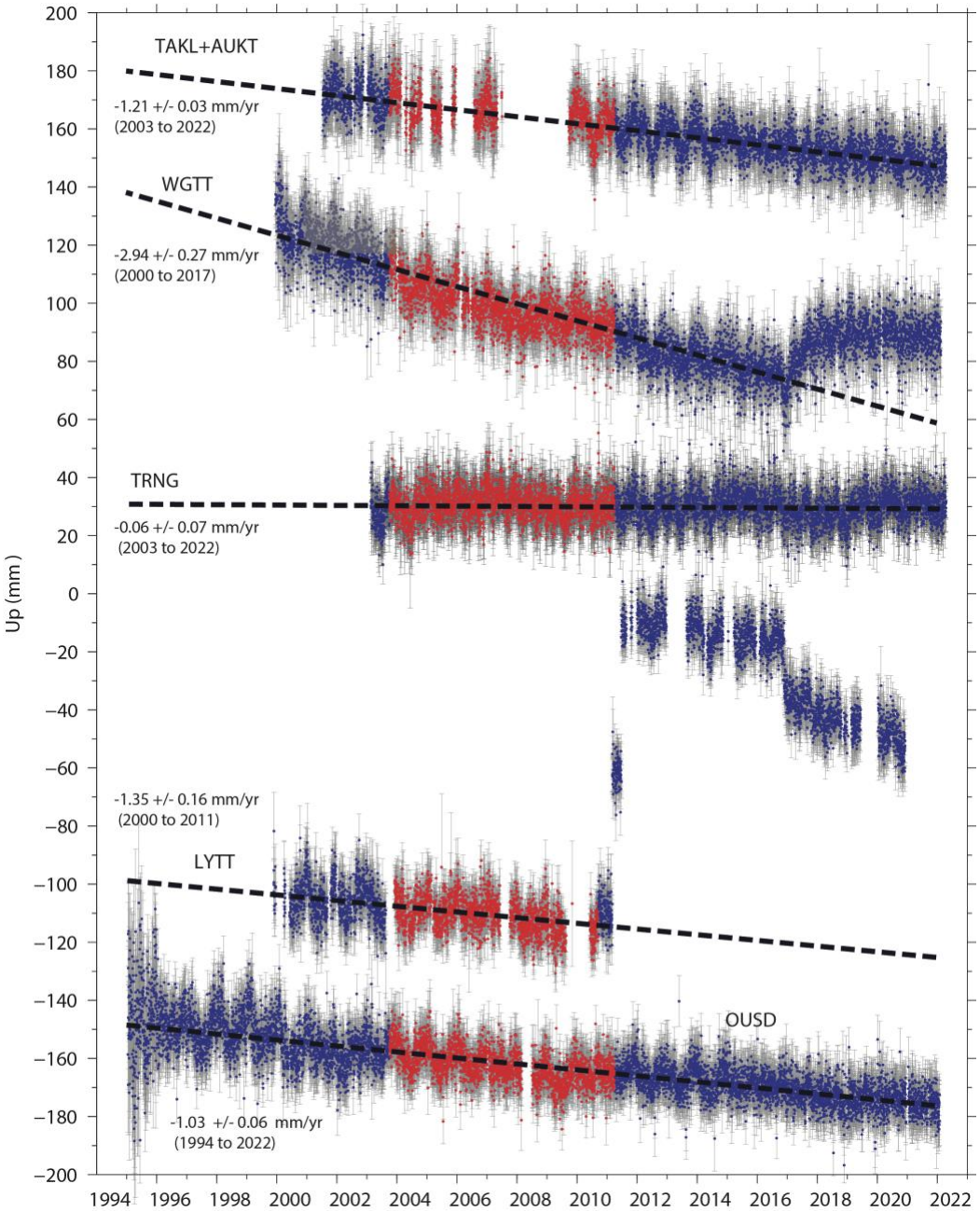

Figure 7. Time series and interseismic rates of VLM for cGNSS stations located near five New Zealand tide gauges (TAKL + AUKT – Auckland TG, WGTT – Wellington TG, TRNG – closest to Moturiki, LYTT – Christchurch/Lyttleton TG, OUSD – Dunedin TG). Red = interseismic InSAR period 2003-2011. Black dashed line = interseismic trend.

565 4.3 An example of regional-scale variation in RSL projections.
566
567 High resolution spatial coverage offered by our InSAR and GNSS analysis reveals that vertical
568 land movement can vary significantly across short distances in many coastal regions. These short
569 wavelength variations can be attributed to a range of processes including local tectonics,
570 postseismic relaxation, sediment compaction, and anthropogenic factors such as groundwater
571 extraction. The effects of the interplay between these processes are clearly illustrated along the
572 Hawkes Bay coastline between Cape Kidnappers and the region around Napier (Fig. 8). Here rates
573 of VLM vary by ~5 mm across 22 km along the coast from Te Awanga (-0.2 mm y^{-1}) to Ahuriri (-
574 4.73 mm y^{-1}). This spatial pattern is nearly the inverse of the uplift and subsidence that occurred
575 in the 1931 Mw7.4 Hawke's Bay earthquake where uplift of ~1.5 m occurred at Ahuriri and
576 subsidence of ~0.5 m occured near Clive (Hull, 1990). The correspondence of these vertical
577 deformation patterns could imply the coastline is still responding to the sudden coseismic changes
578 of 1931 through postseismic relaxation, however given the magnitude of the 1931 earthqauke and
579 the depth to mantle, other processes such as groundwater removal and compact seem more likely.
580 Compounding this pattern may be ongoing compaction of the Holocene fluvial and estuarine
581 sediments that infill the former Ahuriri Lagoon, and the pre-1931 lagoon and swamp areas that
582 underlie much of the suburban areas of modern Napier. Ongoing groundwater extraction from
583 aquifers underlying the Heretaunga Plains could also be amplifying the subsidence. The near stable
584 VLM rates near Cape Kidnappers may be due to a less-compressible substrate (fluvial gravel-
585 dominated rather than the silt and peat layers that underlie Ahuriri Lagoon), distance from areas
586 of more intense groundwater extraction, and localised uplift on on reverse faults that lie just
587 offshore Cape Kidnappers block (Barnes et al., 2010).
588
589 The pattern of differential vertical deformation across the Cape Kidnappers to Ahuriri transect also
590 mirrors longer term tectonic signals. Ahuriri Lagoon has a geological record of Holocene
591 subsidence with up to 7 earthquakes in the past 7300 years creating 8-10 m of net subsidence
592 (Hayward et al., 2015; Hayward et al., 2016). Uplift in the 1931 earthquake was an anomaly within
593 the longer term context. In contrast the Clive to Waimarama coast, including Cape Kidnappers,
594 has a Holocene history of earthquakes that have caused uplift (Hull, 1987) and ~125ka Pleistocene
595 marine terraces lie at up to 200 m elevation.
596
597 These variations in VLM have a significant effect on sea level projections along the relatively
598 short distance across the Hawkes Bay coast. For example, the likely range (17th to 83rd percentile)
599 of RSL at Te Awanga (Site 2242, Fig. 8) for SSP2-2.6 by 2150 is 0.39 m to 1.13 m, while at
600 Ahuriri (Site 2263, Fig. 8) the likely range under the same emissions scenario is 1.05 to 1.76 m.
601 This is a 100% increase or doubling of the median value (0.72 m to1.38 m) due to VLM along.
602 This variability highlights that use of a single set of relative sea level projections for coastal
603 planning in New Zealand is not appropriate, even at a regional scale. These data also suggest that
604 New Zealand's TG records cannot accurately capture regional variations in relative sea level.
605

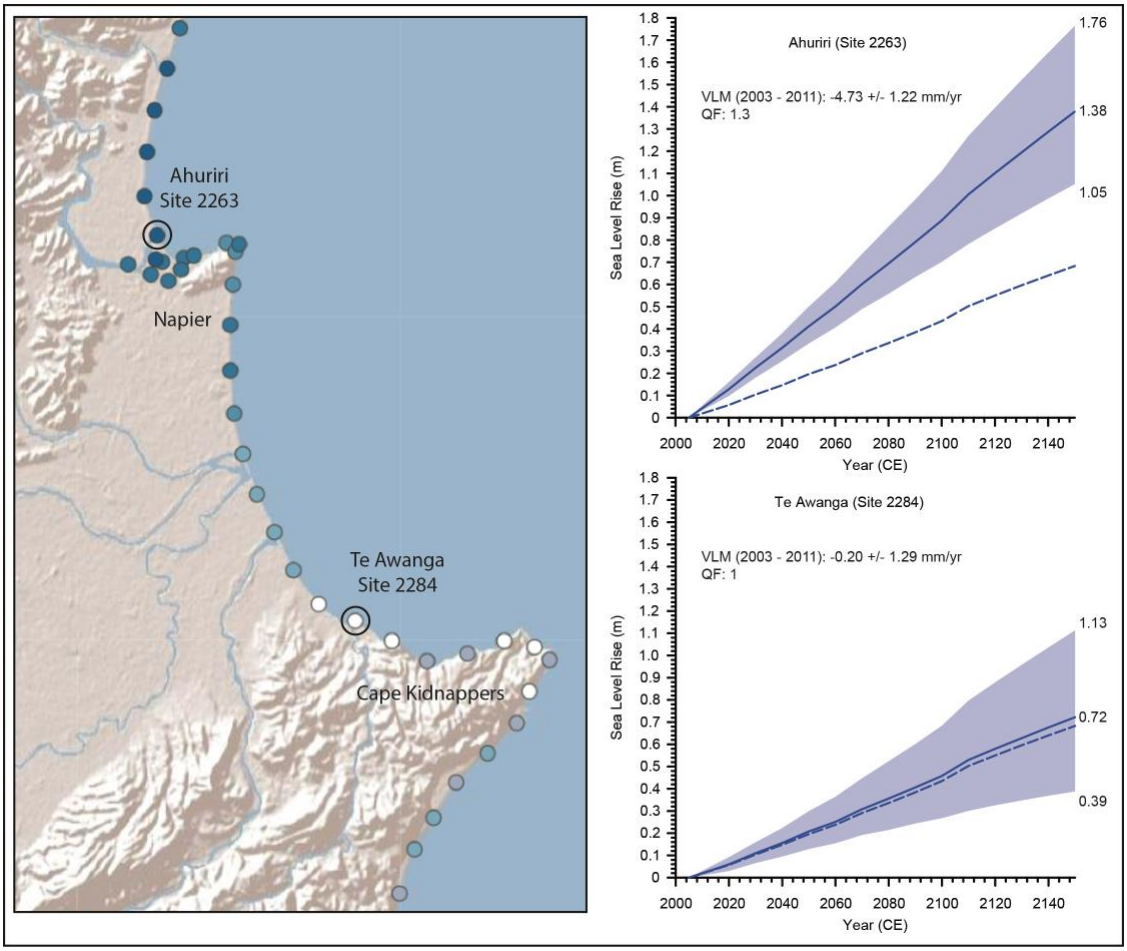

Figure 8. RSL projections (median 13th-87th percentile; medium confidence) to 2150 for (A) Napier Airport - Ahuriri and (B) Haumoana - Te Awanga showing the dramatic variability in VLM influence on the Hawkes Bay coastline for SSP1-2.6. Baseline reference period follows AR6 and is the mean of 1995-2014. QF = quality factor (see Supporting Information).

4.4 Low confidence RSL projections & long-term committment to sea-level rise.

In order to explore the potential influence of low confidence processes, which may lead to rapid, non-linear and self-sustaining collapse of large sectors of the Antarctic ice sheet grounded on bedrock below sea-level, we have plotted *low confidence* (likely 17th-83rd percentile) projections for emission pathways SSP1-2.6 and SSP5-8.5 to 2300 for our highest subsidence and highest uplift sites (Fig. 9). These low confidence processes are currently only incorporated into a single ice sheet model as discussed in sections 2.2 and 3.2, but when this model is incorporated into probabilistic sea-level projections, they provide a plausible upper bound for extreme sea-level rise, which cannot be ruled out.

At the highest subsidence site in the southern Wairarapa coast at Oroi Stream (Figs. 1A, 9; the upper bound (83rd percentile) of RSL rise by 2300 for SSP1-2.6 and SSP5-8.5 is 5.52 m and 17.61 m, respectively. At the highest uplift site on eastern Bay of Plenty coastline near Ohinepanea (Figs. 1A, 9) the upper bound (83rd percentile) of RSL by 2300 for SSP1-2.6 and SSP5-8.5, is 1.81 m

and 14.45 m, respectively. Whereas VLMs significantly amplify or ameliorate RSL rise for the SSP1-2.6 emissions scenario, VLMs are overwhelmed by Antarctic ice sheet loss for higher emissions scenarios by 2300. This is especially the case for SSP5-8.5. We also note that extrapolation of VLMs out to 2300, which are based on interseismic rates, for some parts of the New Zealand coastline will begin to overlap with an increased likelihood of a sesimic event that may reverse the sign and dramaticaaly increase the instantaneous rate of VLM.

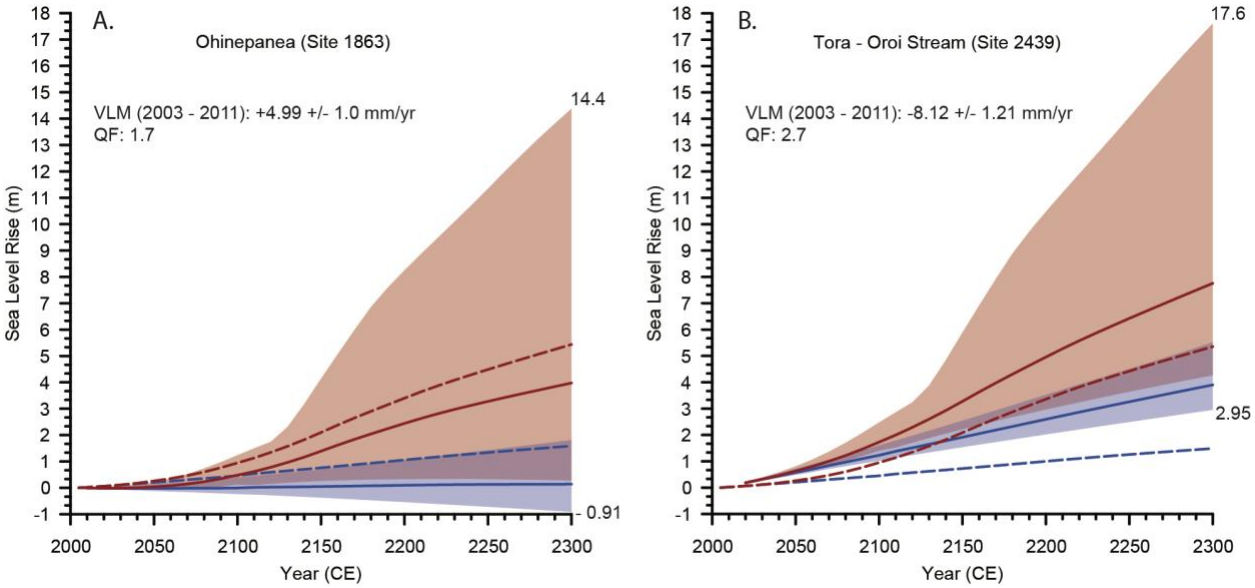

Figure 10. RSL projections (median 17th-83rd percentile; *low confidence*) to 2150 for (A) Tora - Orio Stream, Wairarapa coast and (B) Ohinepanea - Pikowai, Bay of Plenty Coast, showing the influence of VLM for SSP1-2.6 and SSP5-8.5. Baseline reference period follows AR6 and is the mean of 1995-2014. QF = quality factor (see Supporting Information). Dashed lines = no VLM included in projection.

Our results reflect the influence of a tipping point affecting the Antarctic ice sheet, that may be avoided by stabilisation of global warming in line with the Paris Climate Agreement (SSP1-2.6) (DeConto et al., 2021; Golledge et al., 2015). This point appears to be crossed when the majority of Antarctica's stabilising apron of ice shelves is lost allowing unstable and irreversible processes such as MICI and MISI to dominate ongoing ice-mass loss. The potential of this threshold creates deep uncertainty for GMSL estimates beyond 2100 and the commitment to inter-generational sea-level rise.

5. Implications of subsidence for coastal risk assessments and planning

For regions where land subsidence is occurring at rates >2mm yr^{-1} (large parts of New Zealand's coastline), VLM makes a significant contribution to RSL projections for all scenarios out to 2150, bringing forward planning decisions. Beyond 2150 the VLMs become increasingly uncertain, and for higher emissions scenarios, the land ice contribution to global sea-level starts to dominate. Here we discuss the planning implications of our RSL projections, where timing of threshold exceedance can be brought forward by decades in subsiding regions.

659 5.1 Case study 1. Implications for decision-making and planning for more frequent coastal
660 flooding
661
662 The rise in mean sea level of ~0.2 m since 1900 around New Zealand has driven an increase in
663 nuisance, chronic and extreme coastal flooding. There is very high confidence that projected sea-
664 level rise will cause even more frequent coastal flooding in New Zealand before mid-century
665 (Lawrence et al., 2022), which leads to higher cumulative risks over time (Paulik et al., 2020).
666 Improved decision-relevant information can be communicated by outlining how future changes in
667 the frequency of rare coastal flood levels or a specific flood event of the recent past will transpire
668 from the ongoing rise in RSL, e.g., 1% annual exceedance probability (AEP) or a centennial event
669 on average (Rasmussen et al., 2022; Stephens et al., 2018). Tabulated changes in occurrence of an
670 equivalent magnitude 1% AEP event for the recent past have been produced for increments of RSL
671 for the four main New Zealand ports (Parliamentary Commissioner for the Environment, 2015).
672 The analysis shows that previously rare events will occur on an annual basis (on average) with
673 only modest increases in RSL (0.30–0.45 m). This shift in frequency will occur earlier in areas
674 that have small tide ranges as New Zealand coastal flooding is strongly influenced by tidal range
675 (vs. storm-surge dominated) (Stephens et al., 2018).
676
677 Figure 11 shows the impact that VLM has on planning, design and decision-making timelines
678 under SSP2–4.5 RSL projections near three of New Zealand's main ports. These results clearly
679 show that subsidence rates shift adaptation planning timeframes forward. Petone (Lower Hutt)
680 (Fig. 11; top panel) will experience the historical 1% AEP coastal flood occurring every year when
681 RSL rise reaches 0.27 m. A relatively high rate of subsidence rate of –2.86 mm y^{-1} at the Petone
682 means this flood frequency change to annually will occur 17 years earlier than it would without
683 subsidence. A change to a higher frequency of once a month, happens at this site when sea level
684 rises by 0.42 m, which occurs 22 years earlier.. Sites in Kohimarama-Auckland (Fig. 11; mid-
685 panel) and New Brighton-Christchurch (Fig. 11; bottom panel) have lower subsidence rates than
686 Petone, which means the onset of historic rare coastal floods becoming annual and monthly events
687 occur later than in Petone, but sooner than will occur without considering VLM. At New Brighton,
688 with a modest subsidence rate of -0.77 mm.y^{-1}, the change to an annual occurrence (on average)
689 of a past 1% AEP flood is brought forward by only 5 years (9 years to reach a monthly occurrence
690 threshold). However, we note that GNSS measurements at New Brighton show post-earthquake
691 subsidence of ~8 mm y^{-1} for the period 2014-2022 and it is uncertain when or if this suburb will
692 return to its pre-seismic subsidence rate. The New Brighton example highlights the challenge
693 associated with projecting sea level along highly dynamic coastal margins at plate boundaries.
694 Applying an interseismic VLM at New Brighton likely underestimates relative sea-level rise in the
695 near term and may misidentify the time at which flood frequency thresholds will be crossed.
696
697 Importantly, subsidence driven forward shifts in the date at which flood-frequency thresholds are
698 reached are more pronounced for SSP1–2.6 (not shown). Under this lower emissions scenario, the
699 emergence of the annual flood occurrences is brought forward 25, 23 and 9 years respectively for
700 the three urban locations.
701
702

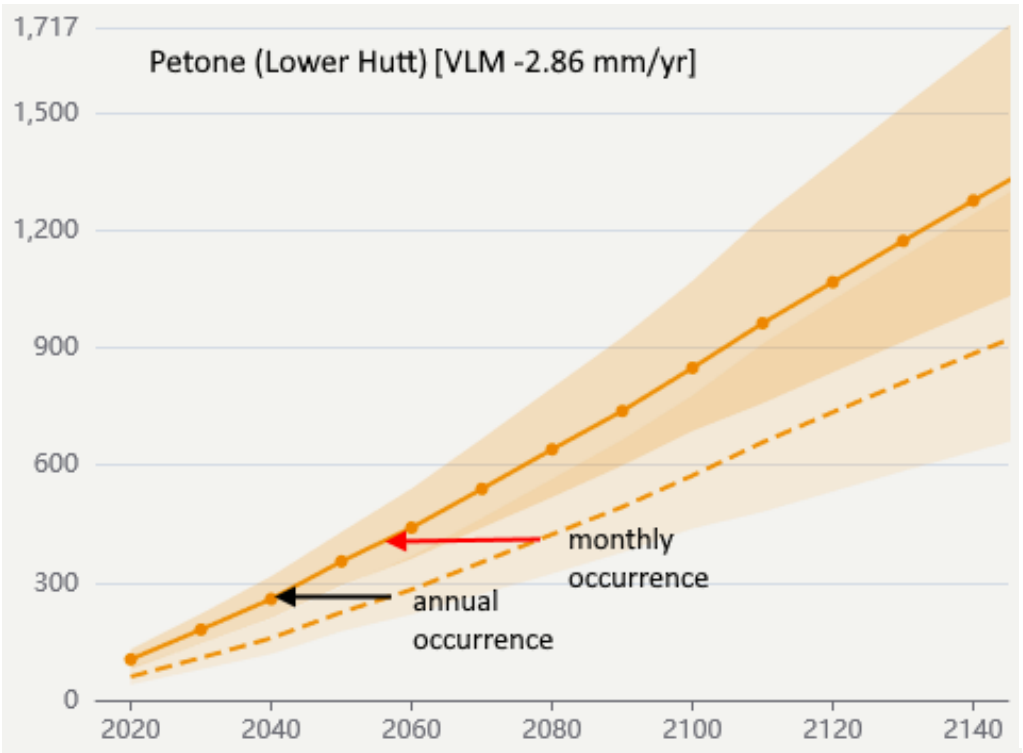
Petone (Lower Hutt) [VLM -2.86 mm/yr]
1,717
1,500
1,200
900
600
300
0
2020
2040
2060
2080
2100
2120
2140
monthly occurrence
annual occurrence

703

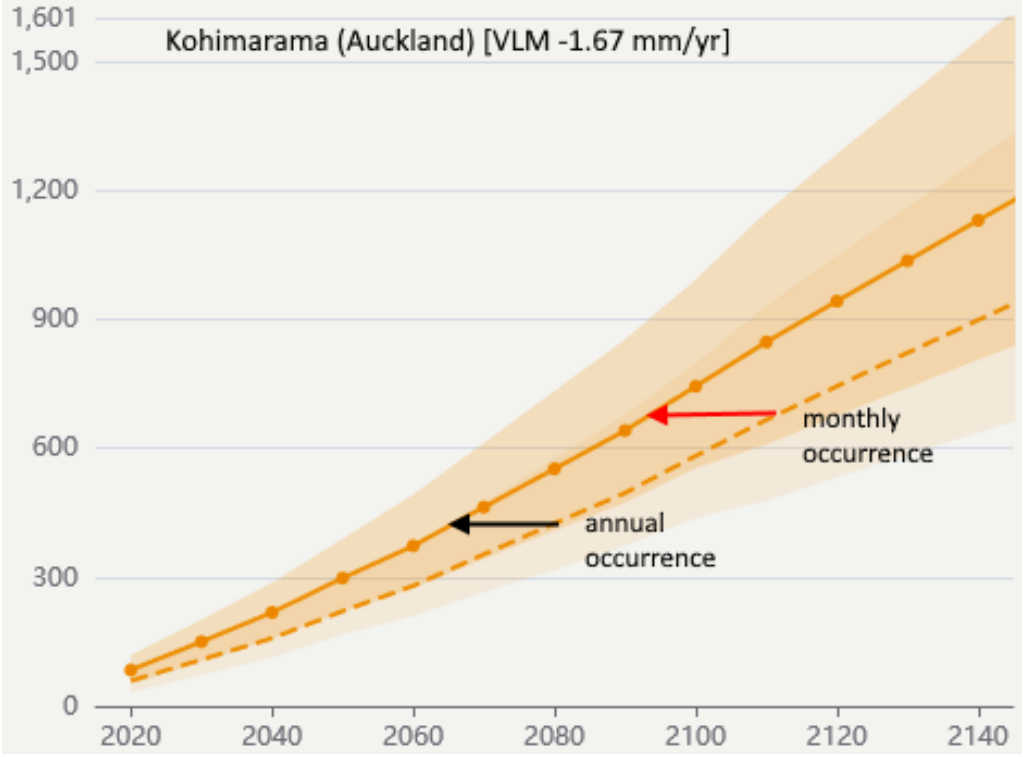
Kohimarama (Auckland) [VLM -1.67 mm/yr]
1,601
1,500
1,200
900
600
300
0
2020
2040
2060
2080
2100
2120
2140
monthly occurrence
annual occurrence

704

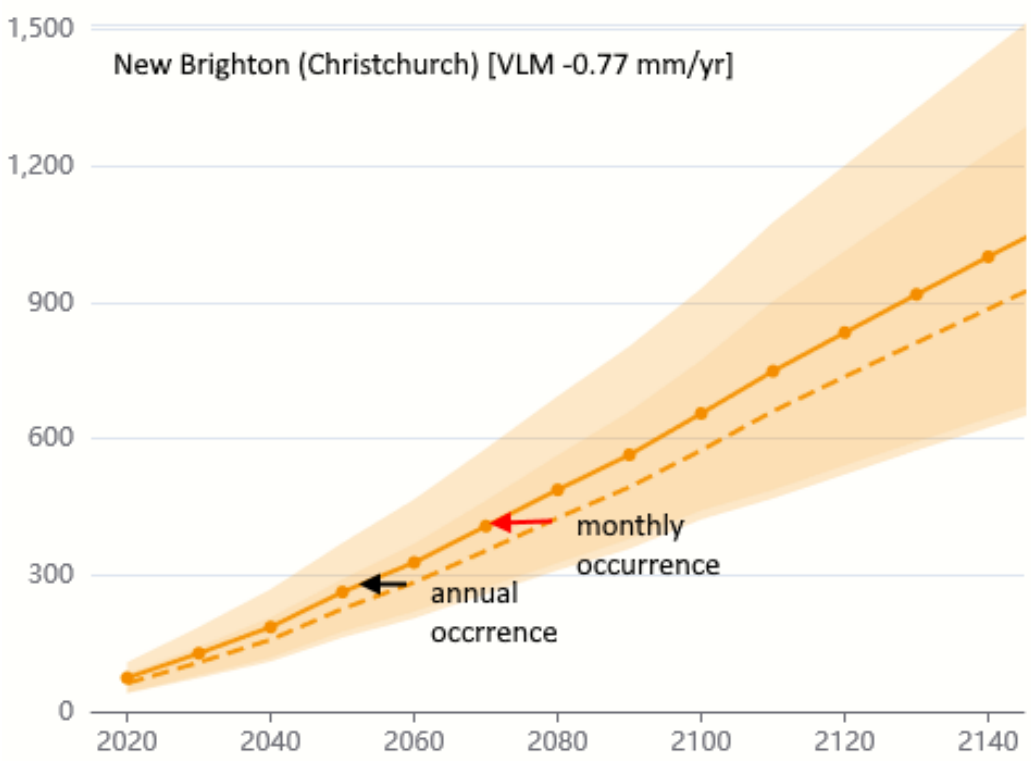

Figure 11: Ocurrences of extreme coastal flooding levels will increase from what used to be a rare 1% AEP event of the recent past, to become more regularly exceeded. Two such flooding thresholds (when annual and monthly occurences occur on average locally) are shown in relation to sea-level rise projections for SSP2–4.5 (median and 17th to 83rd percentile range), both with VLM included (heavy line with markers) and without (dashed line). Sites represent 3 major urban areas in New Zealand where subsidence is present. Inclusion of local subsidence rates brings flood-frequency thresholds forward.

National guidance for coastal adaptation in New Zealand (Lawrence et al., 2018) is framed around a dynamic adaptive pathways planning (DAPP) process that embodies the deepening uncertainty, including when RSL projections encompasse uncertainties in the long-term trends in VLM rates. DAPP is a process through which a series of alternative pathways comprising combinations or sequences of adapation options and planning actions are co-developed with communities (Haasnoot et al., 2021; Lawrence et al., 2018). To guide ongoing implementation of an adaptive strategy derived using DAPP, monitoring indicators of change in risk is essential. Indicators can be tied to early signals (warnings) to inform and enable a switch to the next action on the pathway or to an alternative pathway in a timely manner, before reaching a pre-agreed adaptation threshold, such as intolerable risk or frequency of hazard events (Stephens et al., 2018). Clearly local VLM adjusted RSL projections can shift planning timeframes forward (or backwards) by triggering decision-points in a DAPP strategy earlier (or later). Furthermore, carefully designed monitoring programmes (including ongoing GNSS and InSAR analysis) can be used to assess changes in VLM and update DAPP strategies as time progresses.

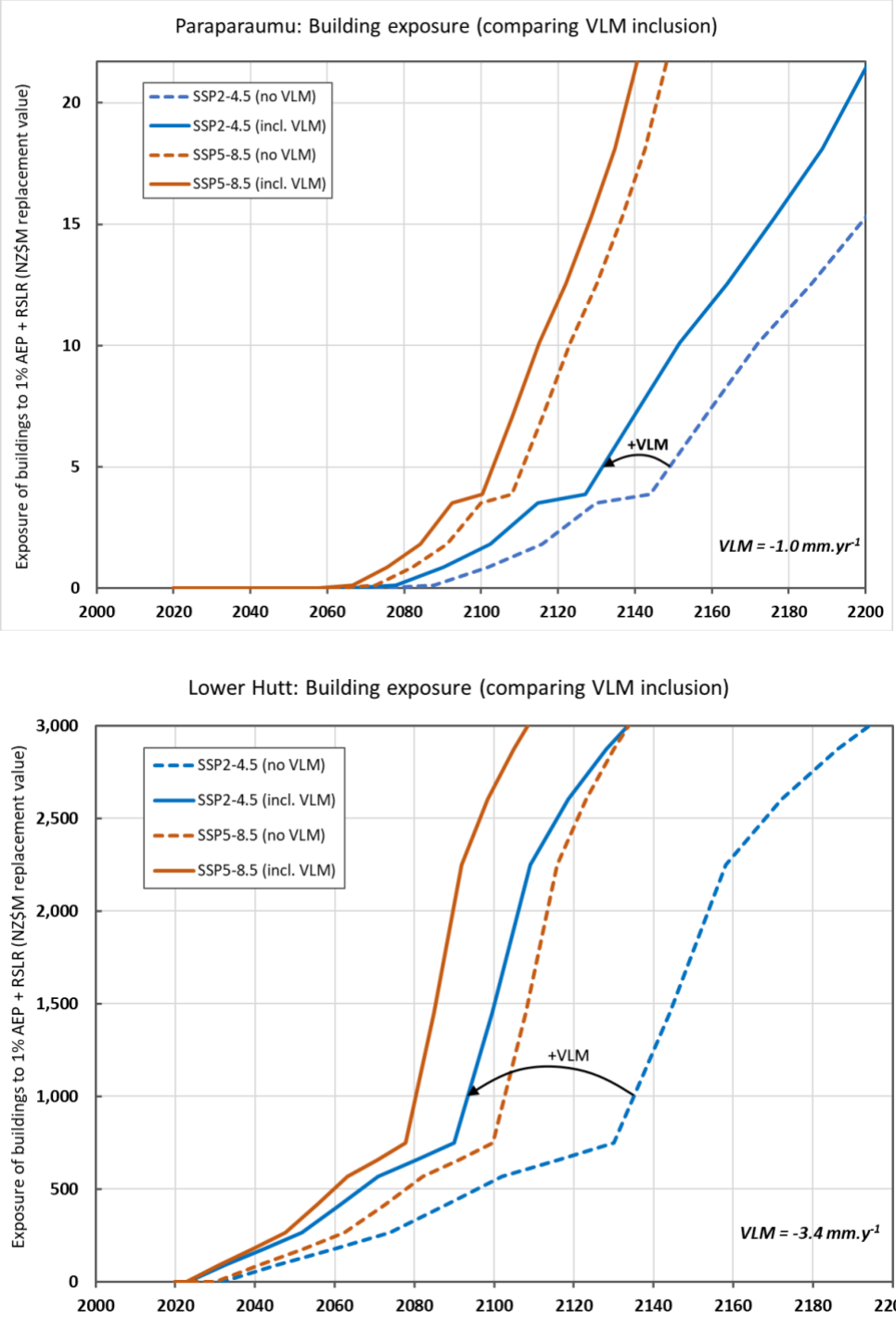

Figure 12: Building replacement value (2021 NZ$M) exposed to 1% AEP coastal flooding and median LSL projections for SSP2-4.5 and SSP5-8.5, with the red lines incoporating average VLM rates of -1.0 mm.y^{-1} (top panel; Paraparaumu) and -3.4 mm.y^{-1} (bottom panel; Lower Hutt).

Case study 2: Implications for risk, damage and loss

To further illustrate the risk, damage and loss effect for RSL projections with different subsidence rates, a static coastal inundation model (only including overland flow with inclusion of levees) was applied in the Wellington region to assess and compare building exposure to present 1% AEP coastal flooding (excluding waves) plus 0.1 m increments of RSL. Here, exposure is expressed as building replacement value (2021 NZD $), calculated on building floor area, storeys and a construction cost index (Paulik et al., 2020). The urban areas of Paraparaumu (~28,000 pop.) and Lower Hutt (~104,000 pop.) were compared using area-averaged VLM subsidence rates of -1.0 and -3.4 mm.y^{-1} respectively. The VLM effect on flood exposure for the two urban areas are shown in Fig. 12, and compare SSP2-4.5 and SSP5-8.5 median projections with and without the VLM subsidence component. Paraparaumu is developed on a cuspate foreland and shows a modest flood exposure increase until 2100 when dune systems are breached by storm-tide flooding. Lower Hutt, built in the late 19th century on a river deltaic system (Kool et al., 2020), exhibits a sharp increase in overland flood exposure (Fig. 12; bottom panel) once RSL exceeds paleo-foredunes from 2080 for the SSP5-8.5 projection.

Local subsidence can significantly shorten planning timeframes for adaptation actions before coastal water level change thresholds are reached. As shown in Fig. 12, land subsidence also hastens flood-risk exposure of built-environments, bringing foward adaptation thresholds. Lower Hutt's high subsidence rate means the SSP2-4.5 RSL projection with VLM, overtakes building exposure for the higher-emissions SSP5-8.5 RSL projection if VLM was not considered (bottom panel; Fig. 12). This highlights the critical role of RSL in informing adaptation planning, compared with only using regional or down-scaled GMSL projections. Conversely, for the Paraparaumu urban area, there is no cross-over of pairs of RSL projections for the two scenarios (with and without VLM) because subsidence is considerably lower than Lower Hutt (-1 mm y^{-1}).

In relation to Lower Hutt, further compound groundwater and hydraulic head effects on stormwater/drainage networks in conjunction with RSL can occur even earlier than by only considering overland flow. Kool et al. (2020) determined a substantially lower adpatation threshold of a 0.3 m RSL rise for stormwater/drainage and wastewater networks in the landward suburbs of Lower Hutt, where the land is low-lying behind the paleo-dune features. Therefore some of the exposure related to building replacement value in Lower Hutt (Fig. 12; bottom panel), would emerge sooner for this lower 0.3 m RSL adaptation threshold because of the limits to the present gravity-based networks. This lower 0.3 m RSL threshold would be reached at ~2043 including VLM for the SSP2-4.5 RSL projection, but two decades later if VLM was not considered.

These examples highlight the need to determine local VLM rates that can inform adaptation guidance for decision makers and infrastructure providers that is cognizant of spatial VLM variability.

5. Concluding remarks

In this study we have used high-resolution vertical velocity data generated for the period 2003-2011 (Hamling et al., 2022) to generate probabilistic RSL projections every 2 km along the coastline of New Zealand. Spatial coverage that was previously limited to our tide gauges (Kopp et al., 2014) has been extended to 7435 sites. We have used the IPCC AR6 approach (Fox-Kemper

et al., 2021; Garner et al., 2021) and present an ensemble of probability distributions of RSL for *medium confidence* processes for Shared Socioeconomic Pathways (SSP) scenarios to 2150 and *low confidence* processes in SSPs to 2300. These new, local "NZSeaRise" projections and underpinning data can be accessed through a web-based GIS-visualisation tool (www.searise.nz/map-2).

Our approach and methodology reveal new insights into the complex role of VLM in projecting future sea level change and impacts and can be applied to any region of the world where the coastline is affected by active tectonic processes. Downward VLM > 2 mm y^{-1} makes a significant contribution to RSL projections for all climate scenarios out to the end of this century bringing forward adaptation planning decision thresholds by decades. In these regions, the influence of VLM on RSL may continue to be significant over the next 300 years but becomes overwhelmed by the accelerating contribution of land ice mass loss. The opposite occurs in regions where land is uplifting, which will experience a slower relative rise in sea-level.

Whereas VLM can vary through time, rates are relatively constant over decadal timescales between large earthquakes. Contemporary subsidence is also prevalent across low lying sedimentary basins around the New Zealand coastline. Here we use the inter-seismic and/or sedimentary basin VLM trend measured from InSAR and GNSS data to produce relative sea level projections at high spatial resolution. However, users of these projections should also consider local seismic hazard risk and known local subsidence hotspots (e.g., historic land reclamation) when planning for coastal adaptation. On timescales longer than the seismic cycle (~100 years), significant sections of New Zealand's coastline are either stable or rising due to the aggregate effect of vertical motion during earthquakes. However, it is important to highlight that 40% of New Zealand's coastline, including the lower North Island and upper South Island, is subsiding over time frames most relevant for planning and decision-making in the near-term (generally before 2050 but out to 100 years).

Uncertainties in VLM rate used in the NZSeaRise projections range from a minimum ± 0.02 mm y^{-1} to maximum ± 5.07 mm y^{-1} and are due to changes in measurement quality at each site. Here we assume that extrapolation of the inter-seismic VLM rate is valid (in lieu of an earthquake) and incorporate VLM measurement uncertainty as part of the full range of uncertainty in relative sea level projections. These additional uncertainties associated with local VLM projections, provides another reason for coastal planners and practitioners to adopt a flexible approach to adaptation (e.g., DAPP). This approach encourages monitoring of VLM alongside other factors that may change risk and allows a shift in adaptation response if VLM changes and becomes a more (or less) significant contributor to future RSL. This new ability to identify the variability that can occur in rates of VLM and hence RSL projections over short stretches of a coastline is very decision relevant for prioritising local adaptation.

Finally, we acknowledge that further work is needed to develop an understanding of the influence of earthquake-cycle related deformation on forecasts of VLM within tectonically active regions around the world. This work should use probabilistic approaches including seismic hazard models and forecasts. There is a need to better assess and quantify uncertainties due to the range of processes that cause short-term temporal variations in VLM at high spatial resolution. This

information is critical to inform coastal planning as communities attempt to adapt to unavoidable sea-level rise. This important work will be the topic of a future study.

Acknowledgements

This work was part of the NZ SeaRise Programme funded by New Zealand Ministry of Business, Innovation & Employment Contract to the Research Trust at Victoria University Contract ID - RTVU1705.

Aspects of TN, NG and RL's contributions were also funded by the New Zealand Antarctic Science Platform Contract - ANTA1801.

We thank the projection authors for developing and making the sea-level rise projections available, multiple funding agencies for supporting the development of the projections, and the NASA Sea-Level Change Team for developing and hosting the IPCC AR6 Sea-Level Projection Tool.

We thank Rebecca Priestley, Ceridwyn Roberts and Zoe Heine and the many stakeholders from New Zealand local government councils, infrastructure provides and Iwi for help with developing, testing and communicating the projections tool.

New Zealand Ministry for the Environment helped support development of the projections tool and their inclusion in the national coastal hazards guidance for local government.

We thank Takiwā for developing and hosting the NZ SeaRise projections website.

We thank Bill Fry, Tim Stern and Simon Lamb for constructive comments that helped improve this paper.

Open Research

The Antarctic Research Centre at Te Herenga Waka: Victoria University of Wellington (ARC), the Institute of Geological and Nuclear Sciences Limited (GNS Science), and the National Institute of Water & Atmospheric Limited (NIWA) have provided data on vertical land movements. The VLM data (Envisat) was collected across the period 2003 to 2011. Sea level projections were made using the FACTs methodology and code published by Garner et al. (2021) and Fox-Kemper et al. (2021) and are available through:

https://zenodo.org/communities/ipcc-ar6-sea-level-projections?page=1&size=20
There are links in that community to the AR6 projection data without VLM contributions (which we later added Ian's data):
https://zenodo.org/record/5967269
As well as the code for producing those projections:
https://zenodo.org/record/6419954
The code for making projections with VLM data are in the FACTS github repository:

https://github.com/radical-collaboration/facts/tree/devel/modules/NZInsarGPS/verticallandmotion

The data, including rates of vertical land movement, errors, quality factors and the sea-level projections, are available for download from https://searise.takiwa.co/map/6245144372b819001837b900/embed.

References

Altamimi, Z., Rebischung, P., Métivier, L., & Collilieux, X. (2016). ITRF2014: A new release of the International Terrestrial Reference Frame modeling nonlinear station motions. *Journal of Geophysical Research: Solid Earth*, *121*(8), 6109-6131.

Bamber, J. L., & Aspinall, W. P. (2013). An expert judgement assessment of future sea level rise from the ice sheets. *Nature Climate Change*, *3*, 424. Article. https://doi.org/10.1038/nclimate1778

Bamber, J. L., Oppenheimer, M., Kopp, R. E., Aspinall, W. P., & Cooke, R. M. (2019). Ice sheet contributions to future sea-level rise from structured expert judgment. *Proceedings of the National Academy of Sciences*, *116*(23), 11195-11200. https://www.pnas.org/content/pnas/116/23/11195.full.pdf

Bamber, J. L., Westaway, R. M., Marzeion, B., & Wouters, B. (2018). The land ice contribution to sea level during the satellite era. *Environmental Research Letters*, *13*(6), 063008. http://dx.doi.org/10.1088/1748-9326/aac2f0

Barnes, P. M., Lamarche, G., Bialas, J., Henrys, S., Pecher, I., Netzeband, G. L., et al. (2010). Tectonic and geological framework for gas hydrates and cold seeps on the Hikurangi subduction margin, New Zealand. *Marine Geology*, *272*(1-4), 26-48.

Beavan, J., Denys, P., Denham, M., Hager, B., Herring, T., & Molnar, P. (2010). Distribution of present-day vertical deformation across the Southern Alps, New Zealand, from 10 years of GPS data. *Geophysical Research Letters*, *37*(16).

Beavan, J., & Litchfield, N. J. (2012). *Vertical Land Movement around the New Zealand Coastline: implications for sea-level rise*. Retrieved from

Beavan, J., Moore, M., Pearson, C., Henderson, M., Parsons, B., Bourne, S., et al. (1999). Crustal deformation during 1994–1998 due to oblique continental collision in the central Southern Alps, New Zealand, and implications for seismic potential of the Alpine fault. *Journal of Geophysical Research: Solid Earth*, *104*(B11), 25233-25255.

Bell, R. G., & Hannah, J. (2019). *Update to 2018 of the annual MSL series and trends around New Zealand. National Institute of Water & Atmospheric Research Ltd, Hamilton, New Zealand*. Retrieved from New Zealand Ministry for the Environment: https://environment.govt.nz/publications/update-to-2018-of-the-annual-msl-series-and-trends-around-new-zealand/

Berryman, K., Ota, Y., Miyauchi, T., Hull, A., Clark, K., Ishibashi, K., et al. (2011). Holocene paleoseismic history of upper-plate faults in the southern Hikurangi subduction margin, New Zealand, deduced from marine terrace records. *Bulletin of the Seismological Society of America*, *101*(5), 2064-2087.

Biggs, J., & Wright, T. J. (2020). How satellite InSAR has grown from opportunistic science to routine monitoring over the last decade. *Nature Communications*, *11*(1), 1-4.

Blewitt, G., Altamimi, Z., Davis, J., Gross, R., Kuo, C.-Y., Lemoine, F. G., et al. (2010). Geodetic observations and global reference frame contributions to understanding sea-level rise and variability. *Understanding sea-level rise and variability*, 256-284.

Burgette, R. J., Weldon, R. J., & Schmidt, D. A. (2009). Interseismic uplift rates for western Oregon and along-strike variation in locking on the Cascadia subduction zone. *Journal of Geophysical Research: Solid Earth*, *114*(B1).

Carbognin, L., & Tosi, L. (2002). Interaction between Climate Changes, Eustacy and Land Subsidence in the North Adriatic Region, Italy. *Marine Ecology, 23*(s1), 38-50. https://onlinelibrary.wiley.com/doi/abs/10.1111/j.1439-0485.2002.tb00006.x

Caron, L., Ivins, E., Larour, E., Adhikari, S., Nilsson, J., & Blewitt, G. (2018). GIA model statistics for GRACE hydrology, cryosphere, and ocean science. *Geophysical Research Letters, 45*(5), 2203-2212.

Cazenave, A., Dominh, K., Ponchaut, F., Soudarin, L., Cretaux, J., & Le Provost, C. (1999). Sea level changes from Topex-Poseidon altimetry and tide gauges, and vertical crustal motions from DORIS. *Geophysical Research Letters, 26*(14), 2077-2080.

Chaussard, E., Amelung, F., Abidin, H., & Hong, S.-H. (2013). Sinking cities in Indonesia: ALOS PALSAR detects rapid subsidence due to groundwater and gas extraction. *Remote Sensing of Environment, 128*, 150-161.

Church, J. A., Clark, P. U., Cazenave, A., Gregory, J. M., Jevrejeva, S., Levermann, A., et al. (2013). Sea Level Change. In T. F. Stocker, D. Qin, G.-K. Plattner, M. Tignor, S. K. Allen, J. Boschung , A. Nauels, Y. Xia, V. Bex, & P. M. Midgley (Eds.), *Climate Change 2013: The Physical Science Basis. Contribution of Working Group I to the Fifth Assessment Report of the Intergovernmental Panel on Climate Change* (pp. 1137-1216): Cambridge University Press, Cambridge, United Kingdom and New York, NY, USA.

Clark, K., Howarth, J., Litchfield, N., Cochran, U., Turnbull, J., Dowling, L., et al. (2019). Geological evidence for past large earthquakes and tsunamis along the Hikurangi subduction margin, New Zealand. *Marine Geology, 412*, 139-172.

Clark, P. U., Shakun, J. D., Marcott, S. A., Mix, A. C., Eby, M., Kulp, S., et al. (2016). Consequences of twenty-first-century policy for multi-millennial climate and sea-level change. *Nature Climate Change, 6*, 360. Perspective. https://doi.org/10.1038/nclimate2923

Collilieux, X., & Wöppelmann, G. (2011). Global sea-level rise and its relation to the terrestrial reference frame. *Journal of Geodesy, 85*(1), 9-22.

Conrad, C. P. (2013). The solid Earth's influence on sea level. *Bulletin, 125*(7-8), 1027-1052.

Dangendorf, S., Hay, C., Calafat, F. M., Marcos, M., Piecuch, C. G., Berk, K., & Jensen, J. (2019). Persistent acceleration in global sea-level rise since the 1960s. *Nature Climate Change, 9*(9), 705-710.

Dangendorf, S., Marcos, M., Wöppelmann, G., Conrad, C. P., Frederikse, T., & Riva, R. (2017). Reassessment of 20th century global mean sea level rise. *Proceedings of the National Academy of Sciences*. http://www.pnas.org/content/early/2017/05/16/1616007114.abstract

DeConto, R. M., Pollard, D., Alley, R. B., Velicogna, I., Gasson, E., Gomez, N., et al. (2021). The Paris Climate Agreement and future sea-level rise from Antarctica. *Nature, 593*(7857), 83-89. https://doi.org/10.1038/s41586-021-03427-0

Denys, P. H., Beavan, R. J., Hannah, J., Pearson, C. F., Palmer, N., Denham, M., & Hreinsdottir, S. (2020). Sea Level Rise in New Zealand: The Effect of Vertical Land Motion on Century-Long Tide Gauge Records in a Tectonically Active Region. *Journal of Geophysical Research: Solid Earth, 125*(1), e2019JB018055. https://agupubs.onlinelibrary.wiley.com/doi/abs/10.1029/2019JB018055

Dixon, T. H., Amelung, F., Ferretti, A., Novali, F., Rocca, F., Dokka, R., et al. (2006). Subsidence and flooding in New Orleans. *Nature, 441*(7093), 587-588.

Douglas, B. C. (2001). Sea level change in the era of the recording tide gauge. In *International Geophysics* (Vol. 75, pp. 37-64): Elsevier.

Edwards, T. L., Nowicki, S., Marzeion, B., Hock, R., Goelzer, H., Seroussi, H., et al. (2021). Projected land ice contributions to twenty-first-century sea level rise. *Nature, 593*(7857), 74-82. https://doi.org/10.1038/s41586-021-03302-y

England, P., & Molnar, P. (1990). Surface uplift, uplift of rocks, and exhumation of rocks. *Geology, 18*(12), 1173-1177.

Erban, L. E., Gorelick, S. M., & Zebker, H. A. (2014). Groundwater extraction, land subsidence, and sea-level rise in the Mekong Delta, Vietnam. *Environmental Research Letters, 9*(8), 084010.

Faccenna, C., & Becker, T. W. (2010). Shaping mobile belts by small-scale convection. *Nature, 465*(7298), 602-605.

Farrell, W., & Clark, J. A. (1976). On postglacial sea level. *Geophysical Journal International, 46*(3), 647-667.

Fox-Kemper, B., Hewitt, H. T., Xiao, C., Aðalgeirsdóttir, G., Drijfhout, S. S., Edwards, T. L., et al. (2021). Ocean, Cryosphere and Sea Level Change. In V. Masson-Delmotte, P. Zhai, A. Pirani, S.L. Connors, C. Péan, S. Berger, N. Caud, Y. Chen, L. Goldfarb, M.I. Gomis, M. Huang, K. Leitzell, E. Lonnoy, J.B.R. Matthews, T.K. Maycock, T. Waterfield, O. Yelekçi, R. Yu, and B. Zhou (Ed.), *Climate Change 2021: The Physical Science Basis. Contribution of Working Group I to the Sixth Assessment Report of the Intergovernmental Panel on Climate Change*. Cambridge University Press.

Frederikse, T., Landerer, F., Caron, L., Adhikari, S., Parkes, D., Humphrey, V. W., et al. (2020). The causes of sea-level rise since 1900. *Nature*, *584*(7821), 393-397. https://doi.org/10.1038/s41586-020-2591-3

Galloway, D. L., & Burbey, T. J. (2011). Regional land subsidence accompanying groundwater extraction. *Hydrogeology Journal*, *19*(8), 1459-1486.

Garner, G. G., T. Hermans, R. E. Kopp, A. B. A. Slangen, T. L. Edwards, A. Levermann, et al. (2021). *IPCC AR6 Sea-Level Rise Projections*. Retrieved from: https://podaac.jpl.nasa.gov/announcements/2021-08-09-Sea-level-projections-from-the-IPCC-6th-Assessment-Report.

Garrett, E., Gehrels, W.R., Hayward, B.W., Newnham, R., Gehrels, M.J., Morey, C.J. and Dangendorf, S. (2022), Drivers of 20th century sea-level change in southern New Zealand determined from proxy and instrumental records. J. Quaternary Sci. https://doi.org/10.1002/jqs.3418

Gerstenberger, M. C., Marzocchi, W., Allen, T., Pagani, M., Adams, J., Danciu, L., et al. (2020). Probabilistic Seismic Hazard Analysis at Regional and National Scales: State of the Art and Future Challenges. *Reviews of Geophysics*, *58*(2), e2019RG000653. https://agupubs.onlinelibrary.wiley.com/doi/abs/10.1029/2019RG000653

Goelzer, H., Nowicki, S., Payne, A., Larour, E., Seroussi, H., Lipscomb, W. H., et al. (2020). The future sea-level contribution of the Greenland ice sheet: a multi-model ensemble study of ISMIP6. *The Cryosphere Discuss.*, *2020*, 1-43. https://tc.copernicus.org/preprints/tc-2019-319/

Golledge, N. R., Kowalewski, D. E., Naish, T. R., Levy, R. H., Fogwill, C. J., & Gasson, E. G. W. (2015). The multi-millennial Antarctic commitment to future sea-level rise. *Nature*, *526*(7573), 421-425. Letter. http://dx.doi.org/10.1038/nature15706

Gornitz, V., Oppenheimer, M., Kopp, R., Orton, P., Buchanan, M., Lin, N., et al. (2019). New York City Panel on Climate Change 2019 Report Chapter 3: Sea Level Rise. *Third international conference on Gas hydrates*, *1439*(1), 71-94. https://nyaspubs.onlinelibrary.wiley.com/doi/abs/10.1111/nyas.14006

Gregory, J. M., Griffies, S. M., Hughes, C. W., Lowe, J. A., Church, J. A., Fukimori, I., et al. (2019). Concepts and Terminology for Sea Level: Mean, Variability and Change, Both Local and Global. *Surveys in Geophysics*, *40*(6), 1251-1289. https://doi.org/10.1007/s10712-019-09525-z

Haasnoot, M., Winter, G., Brown, S., Dawson, R. J., Ward, P. J., & Eilander, D. (2021). Long-term sea-level rise necessitates a commitment to adaptation: A first order assessment. *Climate Risk Management*, *34*, 100355.

Hamling, I. J., D'Anastasio, E., Wallace, L., Ellis, S., Motagh, M., Samsonov, S., et al. (2014). Crustal deformation and stress transfer during a propagating earthquake sequence: The 2013 Cook Strait sequence, central New Zealand. *Journal of Geophysical Research: Solid Earth*, *119*(7), 6080-6092.

Hamling, I. J., Hreinsdóttir, S., Bannister, S., & Palmer, N. (2016). Off-axis magmatism along a subaerial back-arc rift: Observations from the Taupo Volcanic Zone, New Zealand. *Science Advances*, *2*(6), e1600288.

Hamling, I. J., Hreinsdóttir, S., Clark, K., Elliott, J., Liang, C., Fielding, E., et al. (2017). Complex multifault rupture during the 2016 M w 7.8 Kaikōura earthquake, New Zealand. *Science*, *356*(6334), eaam7194.

Hamling, I. J., Wright, T. J., Hreinsdóttir, S., & Wallace, L. M. (2022). A Snapshot of New Zealand's Dynamic Deformation Field From Envisat InSAR and GNSS Observations Between 2003 and 2011. *Geophysical Research Letters*, *49*(2), e2021GL096465. https://agupubs.onlinelibrary.wiley.com/doi/abs/10.1029/2021GL096465

Hamlington, B. D., Frederikse, T., Nerem, R. S., Fasullo, J. T., & Adhikari, S. (2020). Investigating the acceleration of regional sea level rise during the satellite altimeter era. *Geophysical Research Letters*, *47*(5), e2019GL086528.

Hamlington, B. D., Thompson, P., Hammond, W. C., Blewitt, G., & Ray, R. (2016). Assessing the impact of vertical land motion on twentieth century global mean sea level estimates. *Journal of Geophysical Research: Oceans*, *121*(7), 4980-4993.

Han, Y., Zou, J., Lu, Z., Qu, F., Kang, Y., & Li, J. (2020). Ground deformation of wuhan, china, revealed by multi-temporal insar analysis. *Remote Sensing*, *12*(22), 3788.

Hannah, J., & Bell, R. G. (2012). Regional sea level trends in New Zealand. *Journal of Geophysical Research: Oceans*, *117*(C1).

Hayward, B. W., Grenfell, H. R., Sabaa, A. T., Clark, K. J., Cochran, U. A., & Palmer, A. S. (2015). Subsidence-driven environmental change in three Holocene embayments of Ahuriri Inlet, Hikurangi subduction margin, New Zealand. *New Zealand Journal of Geology and Geophysics*, *58*(4), 344-363.

Hayward, B. W., Grenfell, H. R., Sabaa, A. T., Cochran, U. A., Clark, K. J., Wallace, L., & Palmer, A. S. (2016). Salt-marsh foraminiferal record of 10 large Holocene (last 7500 yr) earthquakes on a subducting plate margin, Hawkes Bay, New Zealand. *Bulletin*, *128*(5-6), 896-915.

Herrera-García, G., Ezquerro, P., Tomás, R., Béjar-Pizarro, M., López-Vinielles, J., Rossi, M., et al. (2021). Mapping the global threat of land subsidence. *Science, 371*(6524), 34-36.

Hoggard, M., White, N., & Al-Attar, D. (2016). Global dynamic topography observations reveal limited influence of large-scale mantle flow. *Nature Geoscience, 9*(6), 456-463.

Holt, W. E., & Haines, A. (1995). The kinematics of northern South Island, New Zealand, determined from geologic strain rates. *Journal of Geophysical Research: Solid Earth, 100*(B9), 17991-18010.

Hornblow, S., Quigley, M., Nicol, A., Van Dissen, R., & Wang, N. (2014). Paleoseismology of the 2010 Mw 7.1 Darfield (Canterbury) earthquake source, Greendale Fault, New Zealand. *Tectonophysics, 637*, 178-190.

Horton, R. M., Gornitz, V., Bader, D. A., Ruane, A. C., Goldberg, R., & Rosenzweig, C. (2011). Climate hazard assessment for stakeholder adaptation planning in New York City. *Journal of Applied Meteorology and Climatology, 50*(11), 2247-2266.

Houlié, N., & Stern, T. A. (2017). Vertical tectonics at an active continental margin. *Earth and Planetary Science Letters, 457*, 292-301.

Howarth, J. D., Barth, N. C., Fitzsimons, S. J., Richards-Dinger, K., Clark, K. J., Biasi, G. P., et al. (2021). Spatiotemporal clustering of great earthquakes on a transform fault controlled by geometry. *Nature Geoscience, 14*(5), 314-320.

Howell, A., & Clark, K. J. (2022). Late Holocene coseismic uplift of the Kaikōura coast, New Zealand. *Geosphere, 18*(3), 1104-1137.

Hull, A. G. (1987). A late Holocene marine terrace on the Kidnappers coast, North Island, New Zealand: some implications for shore platform development processes and uplift mechanism. *Quaternary Research, 28*(2), 183-195.

Hull, A. G. (1990). Tectonics of the 1931 Hawke's Bay earthquake. *New Zealand Journal of Geology and Geophysics, 33*(2), 309-320.

Hussain, E., Wright, T. J., Walters, R. J., Bekaert, D. P., Lloyd, R., & Hooper, A. (2018). Constant strain accumulation rate between major earthquakes on the North Anatolian Fault. *Nature Communications, 9*(1), 1-9.

Ivins, E. R., Dokka, R. K., & Blom, R. G. (2007). Post-glacial sediment load and subsidence in coastal Louisiana. *Geophysical Research Letters, 34*(16).

Jackson, L. P., & Jevrejeva, S. (2016). A probabilistic approach to 21st century regional sea-level projections using RCP and High-end scenarios. *Global and Planetary Change, 146*, 179-189.

Jiang, H., Balz, T., Cigna, F., & Tapete, D. (2021). Land subsidence in Wuhan revealed using a non-linear PSInSAR approach with long time series of COSMO-SkyMed SAR data. *Remote Sensing, 13*(7), 1256.

Johnson, C. S., Miller, K. G., Browning, J. V., Kopp, R. E., Khan, N. S., Fan, Y., et al. (2018). The role of sediment compaction and groundwater withdrawal in local sea-level rise, Sandy Hook, New Jersey, USA. *Quaternary Science Reviews, 181*, 30-42.

Kaiser, A., Holden, C., Beavan, J., Beetham, D., Benites, R., Celentano, A., et al. (2012). The Mw 6.2 Christchurch earthquake of February 2011: preliminary report. *New Zealand Journal of Geology and Geophysics, 55*(1), 67-90.

Katsman, C. A., Sterl, A., Beersma, J., Van den Brink, H., Church, J., Hazeleger, W., et al. (2011). Exploring high-end scenarios for local sea level rise to develop flood protection strategies for a low-lying delta—the Netherlands as an example. *Climatic Change, 109*(3), 617-645.

King, D., Newnham, R., Gehrels, R Clark, K. (2020). Late Holocene sea-level changes and vertical land movements in New Zealand, New Zealand, Journal of Geology and Geophysics, DOI: 10.1080/00288306.2020.1761839.

Kool, R., Lawrence, J., Drews, M., & Bell, R. (2020). Preparing for Sea-Level Rise through Adaptive Managed Retreat of a New Zealand Stormwater and Wastewater Network. *Infrastructures, 5*(11), 92. https://www.mdpi.com/2412-3811/5/11/92

Kopp, R. E., Kemp, A. C., Bittermann, K., Horton, B. P., Donnelly, J. P., Gehrels, W. R., et al. (2016). Temperature-driven global sea-level variability in the Common Era. *Proceedings of the National Academy of Sciences, 113*(11), E1434-E1441.

Kopp, R. E., Mitrovica, J. X., Griffies, S. M., Yin, J., Hay, C. C., & Stouffer, R. J. (2010). The impact of Greenland melt on local sea levels: a partially coupled analysis of dynamic and static equilibrium effects in idealized water-hosing experiments. *Climatic Change, 103*(3), 619-625. https://doi.org/10.1007/s10584-010-9935-1

Kreemer, C., Blewitt, G., & Davis, P. M. (2020). Geodetic evidence for a buoyant mantle plume beneath the Eifel volcanic area, NW Europe. *Geophysical Journal International, 222*(2), 1316-1332.

Lamb, S., & Smith, E. (2013). The nature of the plate interface and driving force of interseismic deformation in the New Zealand plate-boundary zone, revealed by the continuous GPS velocity field. *Journal of Geophysical*

Research: Solid Earth, *118*(6), 3160-3189. https://agupubs.onlinelibrary.wiley.com/doi/abs/10.1002/jgrb.50221

Langridge, R., & Berryman, K. (2005). Morphology and slip rate of the Hurunui section of the Hope Fault, South Island, New Zealand. *New Zealand Journal of Geology and Geophysics, 48*(1), 43-57.

Lawrence, J., B. Mackey, F. Chiew, M.J. Costello, N. Hall, K. Hennessy, et al. (2022). Australasia. In H.-O. Pörtner, D.C. Roberts, M. Tignor, E.S. Poloczanska, K. Mintenbeck, A. Alegría, M. Craig, S. Langsdorf, S. Löschke, V. Möller, A. Okem, & B. Rama (Eds.), *Climate Change 2022: Impacts, Adaptation, and Vulnerability. Contribution of Working Group II to the Sixth Assessment Report of the Intergovernmental Panel on Climate Change.*: Cambridge University Press.

Lawrence, J., Bell, R., Blackett, P., Stephens, S., & Allan, S. (2018). National guidance for adapting to coastal hazards and sea-level rise: Anticipating change, when and how to change pathway. *Environmental Science & Policy, 82*, 100-107. https://www.sciencedirect.com/science/article/pii/S1462901117306068

Levermann, A., Griesel, A., Hofmann, M., Montoya, M., & Rahmstorf, S. (2005). Dynamic sea level changes following changes in the thermohaline circulation. *Climate Dynamics, 24*(4), 347-354.

Levermann, A., Winkelmann, R., Albrecht, T., Goelzer, H., Golledge, N. R., Greve, R., et al. (2020). Projecting Antarctica's contribution to future sea level rise from basal ice shelf melt using linear response functions of 16 ice sheet models (LARMIP-2). *Earth System Dynamics, 11*(1), 35-76.

Lin, N., Kopp, R. E., Horton, B. P., & Donnelly, J. P. (2016). Hurricane Sandy's flood frequency increasing from year 1800 to 2100. *Proceedings of the National Academy of Sciences, 113*(43), 12071-12075. https://www.pnas.org/content/pnas/113/43/12071.full.pdf

Little, T. A., Cox, S., Vry, J. K., & Batt, G. (2005). Variations in exhumation level and uplift rate along the obliqu-slip Alpine fault, central Southern Alps, New Zealand. *Geological Society of America Bulletin, 117*(5-6), 707-723.

Mackey, B. H., & Quigley, M. C. (2014). Strong proximal earthquakes revealed by cosmogenic 3He dating of prehistoric rockfalls, Christchurch, New Zealand. *Geology, 42*(11), 975-978.

Mazzotti, S., & Stein, S. (2007). Geodynamic models for earthquake studies in intraplate North America. *Special Papers-Geological Society of America, 425*, 17.

Meinshausen, M., Nicholls, Z. R. J., Lewis, J., Gidden, M. J., Vogel, E., Freund, M., et al. (2020). The shared socio-economic pathway (SSP) greenhouse gas concentrations and their extensions to 2500. *Geosci. Model Dev., 13*(8), 3571-3605. https://gmd.copernicus.org/articles/13/3571/2020/

Michailos, K., Sutherland, R., Townend, J., & Savage, M. K. (2020). Crustal thermal structure and exhumation rates in the Southern Alps near the central Alpine Fault, New Zealand. *Geochemistry, Geophysics, Geosystems, 21*(8), e2020GC008972.

Milne, G. A., Gehrels, W. R., Hughes, C. W., & Tamisiea, M. E. (2009). Identifying the causes of sea-level change. *Nature Geoscience, 2*(7), 471-478.

Milne, G. A., & Mitrovica, J. X. (1998). Postglacial sea-level change on a rotating Earth. *Geophysical Journal International, 133*(1), 1-19.

Ministry for the Environment. (2017). *Coastal hazards and climate change: Guidance for local government*. Retrieved from http://www.mfe.govt.nz/publications/climate-change/coastal-hazards-and-climate-change-guidance-local-government

Mitrovica, J. X., Gomez, N., Morrow, E., Hay, C., Latychev, K., & Tamisiea, M. E. (2011). On the robustness of predictions of sea level fingerprints. *Geophysical Journal International, 187*(2), 729-742. https://onlinelibrary.wiley.com/doi/abs/10.1111/j.1365-246X.2011.05090.x

Moucha, R., Forte, A. M., Mitrovica, J. X., Rowley, D. B., Quéré, S., Simmons, N. A., & Grand, S. P. (2008). Dynamic topography and long-term sea-level variations: There is no such thing as a stable continental platform. *Earth and Planetary Science Letters, 271*(1-4), 101-108.

Müller, R., Hassan, R., Gurnis, M., Flament, N., & Williams, S. E. (2018). Dynamic topography of passive continental margins and their hinterlands since the Cretaceous. *Gondwana Research, 53*, 225-251.

National Research Council. (2012). *Sea-level rise for the coasts of California, Oregon, and Washington: past, present, and future*: National Academies Press.

Nerem, R. S., Beckley, B. D., Fasullo, J. T., Hamlington, B. D., Masters, D., & Mitchum, G. T. (2018). Climate-change–driven accelerated sea-level rise detected in the altimeter era. *Proceedings of the National Academy of Sciences*. http://www.pnas.org/content/pnas/early/2018/02/06/1717312115.full.pdf

Nicol, A., Mazengarb, C., Chanier, F., Rait, G., Uruski, C., & Wallace, L. (2007). Tectonic evolution of the active Hikurangi subduction margin, New Zealand, since the Oligocene. *Tectonics, 26*(4). https://agupubs.onlinelibrary.wiley.com/doi/abs/10.1029/2006TC002090

Norris, R. J., & Cooper, A. F. (2001). Late Quaternary slip rates and slip partitioning on the Alpine Fault, New Zealand. *Journal of Structural Geology, 23*(2-3), 507-520.

Nowicki, S. M. J., Payne, A., Larour, E., Seroussi, H., Goelzer, H., Lipscomb, W., et al. (2016). Ice Sheet Model Intercomparison Project (ISMIP6) contribution to CMIP6. *Geosci. Model Dev., 9*(12), 4521-4545. https://www.geosci-model-dev.net/9/4521/2016/

Parliamentary Commissioner for the Environment. (2015). *Preparing New Zealand for rising seas: Certainty and Uncertainty*. Retrieved from

Parsons, T. (2021). The Weight of Cities: Urbanization Effects on Earth's Subsurface. *AGU Advances, 2*(1), e2020AV000277. https://agupubs.onlinelibrary.wiley.com/doi/abs/10.1029/2020AV000277

Paulik, R., Stephens, S. A., Bell, R. G., Wadhwa, S., & Popovich, B. (2020). National-Scale Built-Environment Exposure to 100-Year Extreme Sea Levels and Sea-Level Rise. . *Sustainability, 12*(1513).

Peltier, W. R., Argus, D., & Drummond, R. (2015). Space geodesy constrains ice age terminal deglaciation: The global ICE-6G_C (VM5a) model. *Journal of Geophysical Research: Solid Earth, 120*(1), 450-487.

Perrette, M., Landerer, F., Riva, R., Frieler, K., & Meinshausen, M. (2013). A scaling approach to project regional sea level rise and its uncertainties. *Earth System Dynamics, 4*(1), 11-29.

Petersen, T., Ristau, J., Beavan, J., Denys, P., Denham, M., Field, B., et al. (2009). The Mw 6.7 George Sound earthquake of October 15, 2007: Response and preliminary results. *Bulletin of the New Zealand Society for Earthquake Engineering, 42*(2), 129-141. https://bulletin.nzsee.org.nz/index.php/bnzsee/article/view/307

Pillans, B. (1986). A late Quaternary uplift map for North Island New Zealand. *Roy. Soc. New Zealand Bull., 24*, 409-417.

Pizer, C., Clark, K., Howarth, J., Garrett, E., Wang, X., Rhoades, D., & Woodroffe, S. (2021). Paleotsunamis on the Southern Hikurangi Subduction Zone, New Zealand, Show Regular Recurrence of Large Subduction Earthquakes. *The Seismic Record, 1*(2), 75-84. https://doi.org/10.1785/0320210012

Poitevin, C., Wöppelmann, G., Raucoules, D., Le Cozannet, G., Marcos, M., & Testut, L. (2019). Vertical land motion and relative sea level changes along the coastline of Brest (France) from combined space-borne geodetic methods. *Remote Sensing of Environment, 222*, 275-285.

Rasmussen, D., Kulp, S., Kopp, R. E., Oppenheimer, M., & Strauss, B. H. (2022). Popular extreme sea level metrics can better communicate impacts. *Climatic Change, 170*(3), 1-17.

Ray, R., Beckley, B., & Lemoine, F. (2010). Vertical crustal motion derived from satellite altimetry and tide gauges, and comparisons with DORIS measurements. *Advances in Space Research, 45*(12), 1510-1522.

Riva, R. E., Frederikse, T., King, M. A., Marzeion, B., & van den Broeke, M. R. (2017). Brief communication: The global signature of post-1900 land ice wastage on vertical land motion. *The Cryosphere, 11*(3), 1327-1332.

Royston, S., Watson, C. S., Legrésy, B., King, M. A., Church, J. A., & Bos, M. S. (2018). Sea-level trend uncertainty with Pacific climatic variability and temporally-correlated noise. *Journal of Geophysical Research: Oceans, 123*(3), 1978-1993.

Ryan, D. D., Clement, A. J., Jankowski, N. R., & Stocchi, P. (2021). The last interglacial sea-level record of Aotearoa New Zealand. *Earth System Science Data, 13*(7), 3399-3437.

Santamaría-Gómez, A., Gravelle, M., Dangendorf, S., Marcos, M., Spada, G., & Wöppelmann, G. (2017). Uncertainty of the 20th century sea-level rise due to vertical land motion errors. *Earth and Planetary Science Letters, 473*, 24-32.

Seroussi, H., Nowicki, S., Payne, A. J., Goelzer, H., Lipscomb, W. H., Abe-Ouchi, A., et al. (2020). ISMIP6 Antarctica: a multi-model ensemble of the Antarctic ice sheet evolution over the 21st century. *The Cryosphere, 14*(9), 3033-3070. https://tc.copernicus.org/articles/14/3033/2020/

Shepherd, A., Ivins, E., Rignot, E., Smith, B., van den Broeke, M., Velicogna, I., et al. (2018). Mass balance of the Antarctic Ice Sheet from 1992 to 2017. *Nature, 558*(7709), 219-222. https://doi.org/10.1038/s41586-018-0179-y

Slangen, A. B. A., Carson, M., Katsman, C. A., van de Wal, R. S. W., Köhl, A., Vermeersen, L. L. A., & Stammer, D. (2014). Projecting twenty-first century regional sea-level changes. *Climatic Change, 124*(1), 317-332. https://doi.org/10.1007/s10584-014-1080-9

Slangen, A. B. A., Katsman, C. A., Van de Wal, R. S. W., Vermeersen, L. L. A., & Riva, R. E. M. (2012). Towards regional projections of twenty-first century sea-level change based on IPCC SRES scenarios. *Climate Dynamics, 38*(5), 1191-1209.

Small, E. E., & Anderson, R. S. (1995). Geomorphically driven late Cenozoic rock uplift in the Sierra Nevada, California. *Science, 270*(5234), 277-281.

Stammer, D., Cazenave, A., Ponte, R. M., & Tamisiea, M. E. (2013). Causes for Contemporary Regional Sea Level Changes. *Annual Review of Marine Science, 5*(1), 21-46. https://www.annualreviews.org/doi/abs/10.1146/annurev-marine-121211-172406

Stephens, S. A., Bell, R. G., & Lawrence, J. (2018). Developing signals to trigger adaptation to sea-level rise. *Environmental Research Letters, 13*(10), 104004.

Stirling, M., McVerry, G., Gerstenberger, M., Litchfield, N., Van Dissen, R., Berryman, K., et al. (2012). National seismic hazard model for New Zealand: 2010 update. *Bulletin of the Seismological Society of America, 102*(4), 1514-1542.

Sutherland, R., Berryman, K., & Norris, R. (2006). Quaternary slip rate and geomorphology of the Alpine fault: Implications for kinematics and seismic hazard in southwest New Zealand. *Geological Society of America Bulletin, 118*(3-4), 464-474.

Van Breedam, J., Goelzer, H., & Huybrechts, P. (2020). Semi-equilibrated global sea-level change projections for the next 10 000 years. *Earth System Dynamics, 11*(4), 953-976.

Van Dissen, R., & Yeats, R. S. (1991). Hope fault, Jordan thrust, and uplift of the seaward Kaikoura Range, New Zealand. *Geology, 19*(4), 393-396.

Velicogna, I., Sutterley, T. C., & van den Broeke, M. R. (2014). Regional acceleration in ice mass loss from Greenland and Antarctica using GRACE time-variable gravity data. *Geophysical Research Letters, 41*(22), 8130-8137. https://agupubs.onlinelibrary.wiley.com/doi/abs/10.1002/2014GL061052

Wallace, L. M. (2020). Slow slip events in New Zealand. *Annual Review of Earth and Planetary Sciences, 48*, 175-203.

Wallace, L. M., & Beavan, J. (2010). Diverse slow slip behavior at the Hikurangi subduction margin, New Zealand. *Journal of Geophysical Research: Solid Earth, 115*(B12).

Wallace, L. M., Beavan, J., Bannister, S., & Williams, C. (2012). Simultaneous long-term and short-term slow slip events at the Hikurangi subduction margin, New Zealand: Implications for processes that control slow slip event occurrence, duration, and migration. *Journal of Geophysical Research: Solid Earth, 117*(B11).

Wallace, L. M., Beavan, J., McCaffrey, R., Berryman, K., & Denys, P. (2007). Balancing the plate motion budget in the South Island, New Zealand using GPS, geological and seismological data. *Geophysical Journal International, 168*(1), 332-352.

Wallace, L. M., Beavan, J., McCaffrey, R., & Darby, D. (2004). Subduction zone coupling and tectonic block rotations in the North Island, New Zealand. *Journal of Geophysical Research: Solid Earth, 109*(B12). https://agupubs.onlinelibrary.wiley.com/doi/abs/10.1029/2004JB003241

Wallace, L. M., Cochran, U. A., Power, W. L., & Clark, K. J. (2014). Earthquake and tsunami potential of the Hikurangi subduction thrust, New Zealand: Insights from paleoseismology, GPS, and tsunami modeling. *Oceanography, 27*(2), 104-117.

Wallace, L. M., Hreinsdóttir, S., Ellis, S., Hamling, I., D'Anastasio, E., & Denys, P. (2018). Triggered Slow Slip and Afterslip on the Southern Hikurangi Subduction Zone Following the Kaikōura Earthquake. *Geophysical Research Letters, 45*(10), 4710-4718. https://agupubs.onlinelibrary.wiley.com/doi/abs/10.1002/2018GL077385

Watson, C., Burgette, R., Tregoning, P., White, N., Hunter, J., Coleman, R., et al. (2010). Twentieth century constraints on sea level change and earthquake deformation at Macquarie Island. *Geophysical Journal International, 182*(2), 781-796.

White, W. A., & Morton, R. A. (1997). Wetland losses related to fault movement and hydrocarbon production, southeastern Texas coast. *Journal of Coastal Research*, 1305-1320.

Wöppelmann, G., & Marcos, M. (2016). Vertical land motion as a key to understanding sea level change and variability. *Reviews of Geophysics, 54*(1), 64-92.

Wöppelmann, G., Miguez, B. M., Bouin, M.-N., & Altamimi, Z. (2007). Geocentric sea-level trend estimates from GPS analyses at relevant tide gauges world-wide. *Global and Planetary Change, 57*(3-4), 396-406.

Yin, J., Schlesinger, M. E., & Stouffer, R. J. (2009). Model projections of rapid sea-level rise on the northeast coast of the United States. *Nature Geoscience, 2*(4), 262-266.